# RENEWABLE ENERGY-POWERED HYBRID NF/FO/RO MEMBRANE SYSTEM FOR BRACKISH WATER DESALINATION

BY

MOHAMMED FAISAL MUSA ABDELMAHMOUD

A Thesis Presented to the
DEANSHIP OF GRADUATE STUDIES

**KING FAHD UNIVERSITY OF PETROLEUM & MINERALS**

DHAHRAN, SAUDI ARABIA

In Partial Fulfillment of the
Requirements for the Degree of

# MASTER OF SCIENCE

In

MECHANICAL ENGINEERING

MAY 2018

KING FAHD UNIVERSITY OF PETROLEUM & MINERALS

DHAHRAN- 31261, SAUDI ARABIA

**DEANSHIP OF GRADUATE STUDIES**

This thesis, written by **MOHAMMED FAISAL MUSA ABDELMAHMOUD** under the direction of his thesis advisor and approved by his thesis committee, has been presented and accepted by the Dean of Graduate Studies, in partial fulfillment of the requirements for the degree of **MASTER OF SCIENCE IN MECHANICAL ENGINEERING.**

Dr. Fahad Al-Sulaiman
(Advisor)

Dr. Zuhair Mattoug Gasem
Department Chairman

Dr. Esmail M. A. Mokhaimer
(Member)

Dr. Salam A. Zummo
Dean of Graduate Studies

Dr. Mohamed A. Antar
(Member)

25/9/18

Date

To all those who helped make this work possible

# ACKNOWLEDGMENTS

First of all, I'd like to say: Alhamdullilah. My appreciation goes to KFUPM for this opportunity I was given, all the knowledge I earned and the beautiful moments I had.

I'd also like to thank my advisor Dr. Fahad Al-Sulaiman for his guidance, encouraging words and patience not only as I worked on this thesis but during the entire time I spent at KFUPM. My deepest gratitude is extended to Dr. Esmail Mokhaimer and Dr. Mohamed Antar for their time and valuable input towards this work.

# TABLE OF CONTENTS

# LIST OF TABLES

# LIST OF FIGURES

# LIST OF ABBREVIATIONS

# ABSTRACT

Full Name : MOHAMMED FAISAL MUSA ABDELMAHMOUD

Thesis Title : RENEWABLE ENERGY-POWERED HYBRID NF/FO/RO MEMBRANE SYSTEM FOR BRACKISH WATER DESALINATION

Major Field : Mechanical Engineering

Date of Degree : May 2018

Water desalination is an important and effective way to meet the increasing demand for freshwater and as a solution to supplement freshwater resources. The major drawback of the current desalination technologies is their high-energy consumption. The desalination processes can be broadly classified into thermal and membrane technologies.

Membrane desalination is one of the desalination technologies that has a high share of the installed capacity of desalination plants worldwide. This technology has always been associated with relatively low energy requirement.

The main objective of the current research work is to evaluate the performance and economic feasibility of an NF/FO/RO hybrid system powered by solar PV and wind energies under the weather conditions of Saudi Arabia.

This work started with modeling the performance of the NF/FO/RO system using EES. The performance parameters were validated against published work in the literature. The most important parameter in the modeling process was the specific power consumption of the membrane system. The specific power consumption was 2.3, 2.48, and 2.76 $kWh/m^3$ corresponding to water salinities of 3000, 6000, and 10000 mg/l respectively.

The specific power consumption of the membrane system was then used to determine the power required to produce certain amounts of water in three locations in Saudi Arabia. Proposed renewable energy systems were simulated in HOMER software to assess their performance and determine all the feasible system combinations.

The best combination of all the feasible combinations was determined based on the cost of energy resulting from that combination. For the location in Wadi Dawasir the best configuration is Diesel/Wind producing electricity at a rate of 0.086 $/kWh, while in Qassim and Tabuk Diesel/PV is the best option resulting in electricity cost of 0.091 and 0.087, respectively. These best combinations were also compared with the best combination in the category that includes all power sources (Diesel/Wind/PV) at all three locations.

The monthly average electricity production of each location is presented along with the fraction of renewable energy used in each system at Wadi Dawasir, Qassim, and Tabuk, which are 57, 4, and 7%, respectively. The resultant drop in gas emissions at Wadi Dawasir, Qassim, and Tabuk for the combined systems compared to the case when only diesel is used is 45, 7, and 9%, respectively. The cash flow summary for the components of each combination was obtained and is presented.

The product water cost was also estimated for the systems in Wadi Dawasir, Qassim, and Tabuk, which was found to be 0.61, 0.56, and 0.55 $/$m^3$, respectively.

An optimization was conducted for the NF system alone and for the overall hybrid membrane system. The best operating conditions (at the lowest specific energy consumption) were determined.

# ملخص الرسالة

**الاسم الكامل: محمد فيصل موسى عبدالمحمود**

**عنوان الرسالة: نظام غشائي هجين (NF/FO/RO) يعمل بالطاقة الشمسية لتحلية الماء منخفض الملوحة**

**التخصص: الهندسة الميكانيكية**

**تاريخ الدرجة العلمية: مايو 2018**

عملية تحلية المياه هي طريقة مهمة وفعالة لمقابلة الطلب المتزايد على المياه النقية وكحل لتناقص موارد المياه العذبة. أكبر جانب سلبي للتقنيات المستخدمة في تحلية المياه هو الاستهلاك العالي للطاقة الذي يؤدي بدوره لارتفاع تكلفة الماء المنتج. يمكن تصنيف التقنيات المستخدمة في تحلية المياه الى تقنيات حرارية وتقنيات تستخدم الأغشية.

تحلية المياه باستخدام الأغشية هي احدى طرق تحلية المياه التي لها نصيب كبير من السعة الكلية لمحطات المياه التي تم انشائها على مستوى العالم. تمتاز هذه التقنية بانخفاض نسبي في استهلاك الطاقة.

الهدف الرئيس لهذا البحث هو دراسة نظام تحلية مياه غشائي هجين (NF/FO/RO) يعمل بالطاقات المتجددة (طاقة الشمس وطاقة الرياح) بالتركيز على الأداء والجدوى الاقتصادية لكذا نظام بأخذ الظروف الجوية وتوفر الطاقات المتجددة في المملكة العربية السعودية في الحسبان.

تم أولا في هذا البحث عمل نموذج رياضي للنظام الغشائي الهجين باستخدام برنامج حل المعادلات الهندسية .(EES) تم التحقق من صحة معاملات الأداء بمقارنة نتائج النموذج الرياضي بأخرى منشورة في عمل سابق. كان أهم معاملات الأداء التي تم التحقق منها كان استهلاك نظام الغشاء النسبي للطاقة. من نتائج النموذج الرياضي ان كان الاستهلاك النسبي للطاقة 2.3، 2.48، و2.76 (kWh/m3) لثلاثة مواقع مقترحة ذات ملوحة 3000، 6000 و10000 (mg/l) على التوالي.

بعد ذلك تم استخدام الاستهلاك النسبي للطاقة للنظام الغشائي الهجين في تحديد الطاقة المطلوبة لإنتاج كمية معلومة من الماء في المواقع الثلاثة المقترحة في المملكة العربية السعودية. تم عمل نماذج لأنظمة طاقة بديلة هجين باستخدام برنامج(HOMER) لدراسة أنظمة الطاقة وتمت محاكاة أداء كل منها وتحديد أيها ذو أعلى جدوى من بين كل التراكيب الممكنة.

بعد أن تم الحصول على كل التراكيب المجدية اقتصاديا تم اختيار أفضلها اعتمادا على أيها اقل استهلاكا للطاقة. للموقع المقترح في وادي الدواسر كانت أفضل تركيبة هي ديزل/رياح والتي انتجت كهرباء بكلفة 0.086 ($/kWh) بينما في الموقعين المقترحين في كل من القصيم وتبوك كانت تكلفة انتاج الكهرباء 0.091 و0.087 ($/kWh) على التوالي. أيضا تمت مقارنة هذه التركيبات بأفضل تركيبة تحتوي على ديزل/رياح/طاقة شمسية في كل المواقع المقترحة.

تم عرض متوسط انتاج الكهرباء الشهري لكل من التركيبات المقترحة كما تم عرض نسبة مشاركة الطاقات المتجددة في الطاقة الكهربائية الكلية المنتجة التي كانت 57، 4 و7% على التوالي. أيضا تمت مقارنة نسبة الانخفاض في انبعاثات الغازات من التركيبات المثلى مع تلك الناتجة من نظام طاقة يستخدم الديزل فقط وكانت 45، 7 و9% للمواقع المقترحة في وادي الدواسر، القصيم وتبوك على التوالي. أخيرا، تم عرض مخطط التدفق النقدي لمكونات كل من التركيبات المثلى.

تم أيضا حساب تكلفة إنتاج الماء للأنظمة المحددة في وادي الدواسر، القصيم وتبوك ووجد أنها 0.61، 0.56 و0.55 ($/m$^3$) على التوالي.

تم أخيرا اختيار حالتين وتم عمل أمثلة لهما لإيجاد ظروف التشغيل التي ينتج عنها أقل استهلاك نسبي للطاقة. الحالة الأولى كانت لنظام NF لوحده والثانية لكامل النظام الغشائي الهجين.

# CHAPTER 1

# INTRODUCTION

## 1.1 Water Crisis

Water is one of the most basic needs for the survival of mankind. Most of the great human civilizations of the past were located by or near water resources. For a long time, available freshwater was in abundance and enough for the human population. With increasing population and decreasing water resources, this is not the case anymore. Freshwater is needed for human domestic use, agriculture, and industry. Figure 1 shows a breakdown of the freshwater use [1].

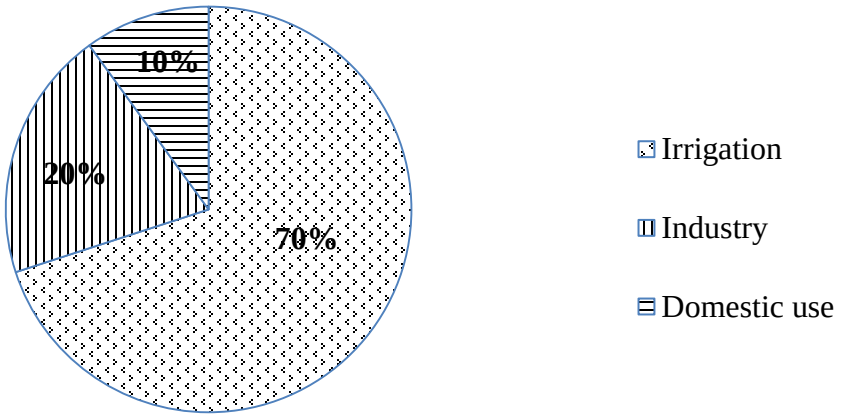


**Figure 1 Global freshwater use**

The world has witnessed a continuous increase in the freshwater demand over the past years at a rate requiring suitable alternative ways to meet the human needs of freshwater.

This need for freshwater can be partially met by means of water conservation and improved catchment and distribution systems.

## 1.2 Water Desalination

Water desalination is an answer to the scarcity of freshwater. However, the energy requirements (cost) of current desalination technologies and the associated negative environmental impact through $CO_2$ emissions and by-products must be considered if the process of freshwater production is to be made sustainable and environment friendly.

The industrial desalination technologies used today can be broadly divided into thermal technologies and membrane technologies. Thermal technologies include technologies such as multistage flashing, multiple effect evaporation, single effect evaporation, freezing, HDH, and solar stills, which is the oldest technique man have used. On the other hand, membrane technologies include electrodialysis, electrodialysis reversal, reverse osmosis, and forward osmosis [2]. Other technologies that does not fit into these two categories include membrane distillation, vacuum distillation, gas hydrates, and ion exchange [3].

## 1.3 Membrane Desalination

Water desalination technologies can be divided into thermal processes and membrane processes. The available membrane processes for desalination include reverse osmosis, nanofiltration (NF), and electrodialysis (ED).

The phenomenon upon which the membrane desalination technologies are built is osmosis. It is a natural phenomenon that was put into use for desalination to help solve the water

scarcity problem after it was proven to be competitive to conventional desalination technologies, i.e., thermal technologies.

Osmosis phenomenon

Osmosis is the natural flow of the water molecules from the low concentration side of a membrane to the higher concentration side. This can be attributed to the higher chemical potential (water concentration or the mole fraction) of water on the side of lower concentration. As a result, a driving force for permeation will exist causing the water to flow from the side with a lower concentration through the membrane.

Osmotic pressure

Osmotic pressure is the pressure difference of liquids on the two sides of a membrane at chemical equilibrium (no water flux across the membrane). In other words, it can be defined as the pressure required to prevent the fresh water from flowing through a membrane towards the side with a higher salt concentration. Osmotic pressure of water is about 2300-2600 kPa and can reach 3500 kPa.

### 1.3.1 Reverse Osmosis

Reverse osmosis (RO) is the process of desalting seawater or brackish water by applying pressure (using a pump) on it forcing water to pass through a membrane that is semi permeable to water and not the salts, with no distinct pores. For the water to pass through the RO membrane, it must follow a complex pathway inside the polymer material of the membrane. The water that passes through the membrane is the product. Figure 2 illustrates both osmosis and reverse osmosis.

Operation principle

RO membranes are operated by applying a hydrostatic pressure that is higher than the solution's osmotic pressure. The resulting positive pressure difference will generate a chemical gradient (the difference in the water molar fraction between the two sides of the membrane) that will cause the water molecules to flow through the membrane against the direction governed by natural osmosis. Most of the salts in the water will be filtered while some will pass through the membrane. The amount of salts passing through the membrane increases with the salt concentration and water temperature [4]. Figure 3 summarizes the principle of RO membranes.

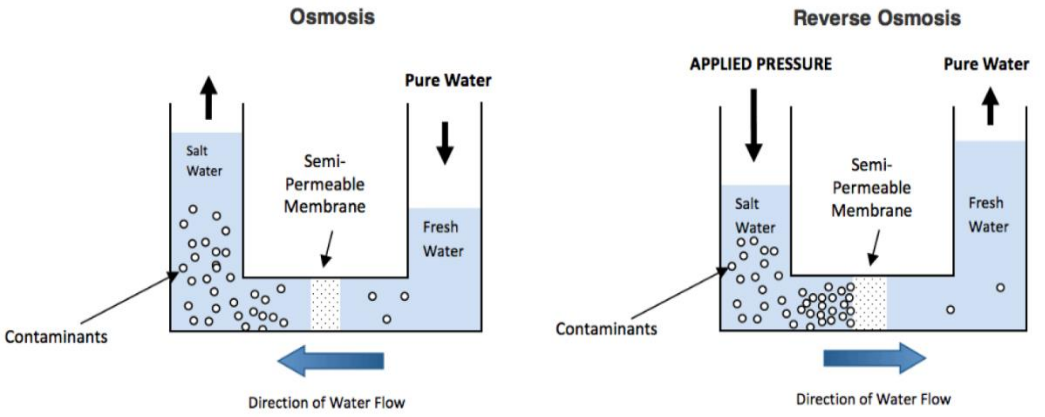


**Figure 2 Osmosis and reverse osmosis**

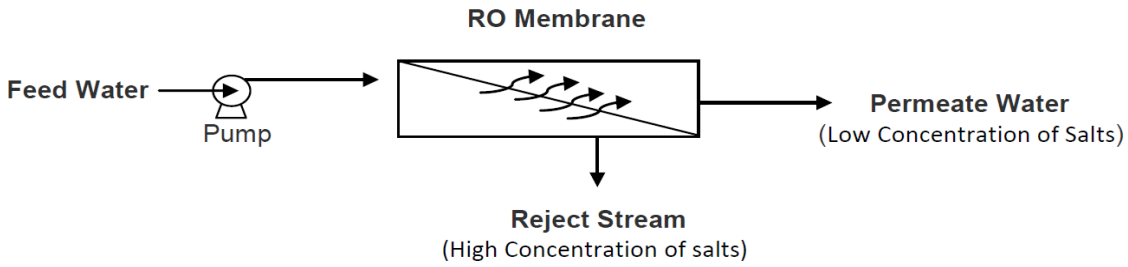


**Figure 3 RO membrane operation principle**

The most important or notable advantages of RO systems over thermal desalination processes are their simplicity and relatively low energy consumption. This has always been one of the reasons behind the increase in the RO desalination market share.

According to Wilf, the RO water production cost dropped from \$2/$m^3$ in 1998 to \$0.5/$m^3$ in 2000, caused by the advances in the technology and the membranes and competition [5]. Figure 4 shows the drop in the water price as reported by Wilf.

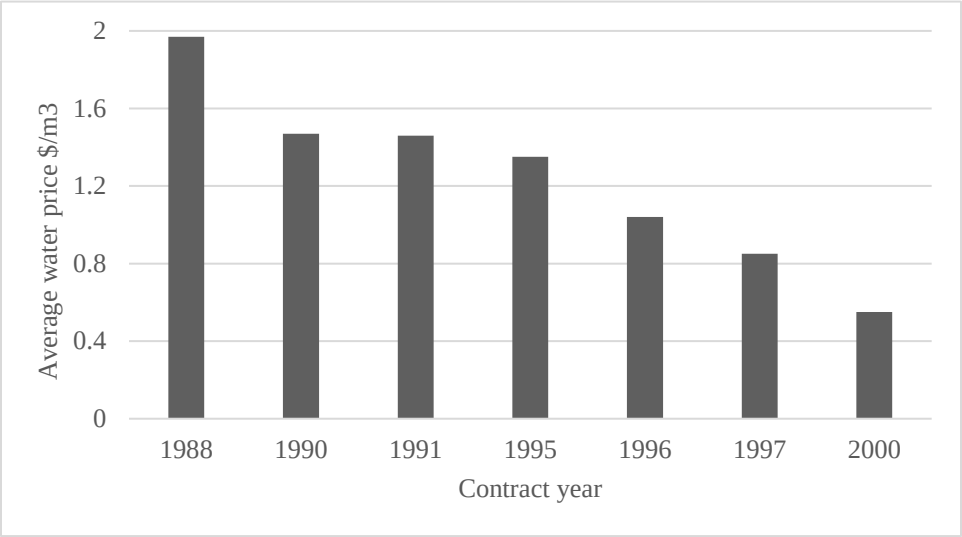


**Figure 4 Water cost for large RO plants**

This cost is shared by various system components, largest being the power and fixed charges. Figure 5 shows the power distribution in a partial double pass system, while Figure 6 shows a breakdown of the cost of water components for a seawater RO plant.

The cost of water production using RO systems can be reduced using hybrid systems employing more than one desalination method or using energy recovery systems. Installing an energy recovery system might lead to a power consumption reduction from 6-8 kWh/$m^3$ to 4-5 kWh/$m^3$ [6].

RO systems run by gas/steam turbines can produce freshwater at rates as low as $\$0.43/m^3$ [7].

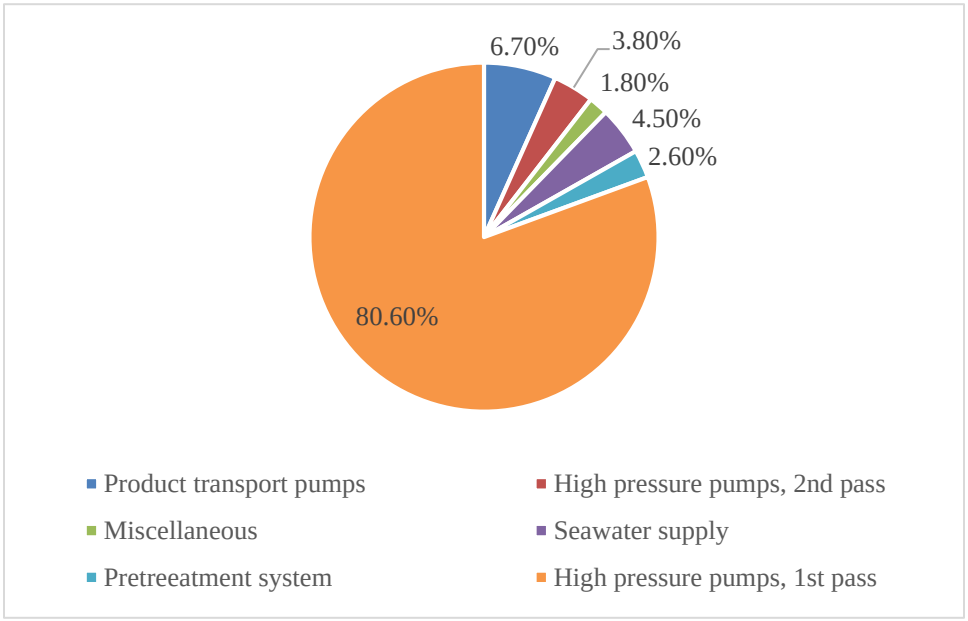


**Figure 5 Double pass RO power usage**

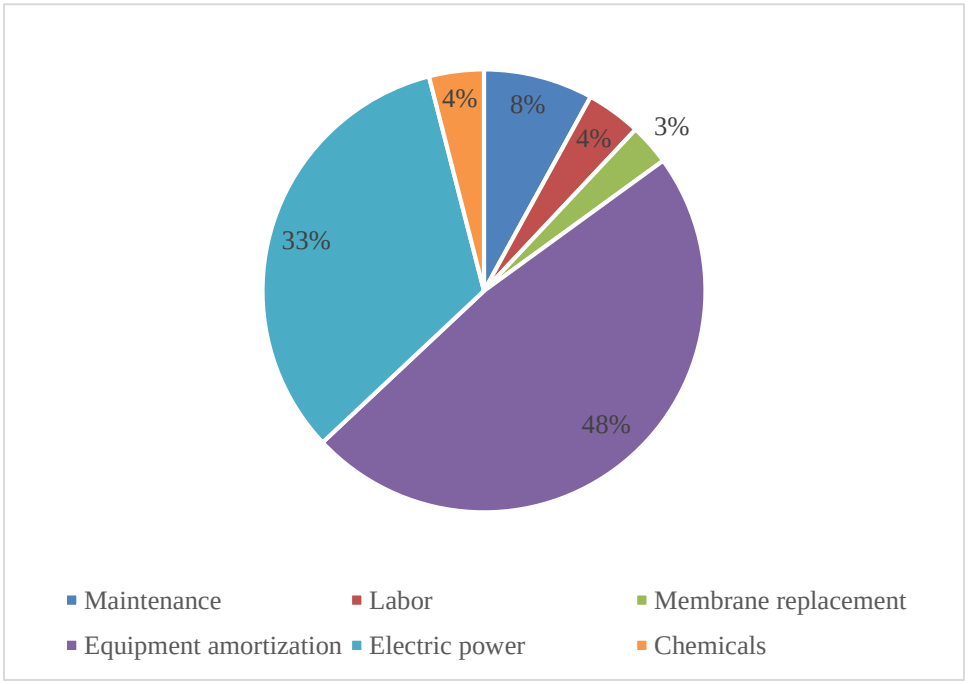


**Figure 6 Seawater RO water cost breakdown**

## RO membrane configurations

The simplest configuration of a single stage RO is shown in Figure 7. The feed water that enters the membrane exits as permeate (product) and concentrate (brine).

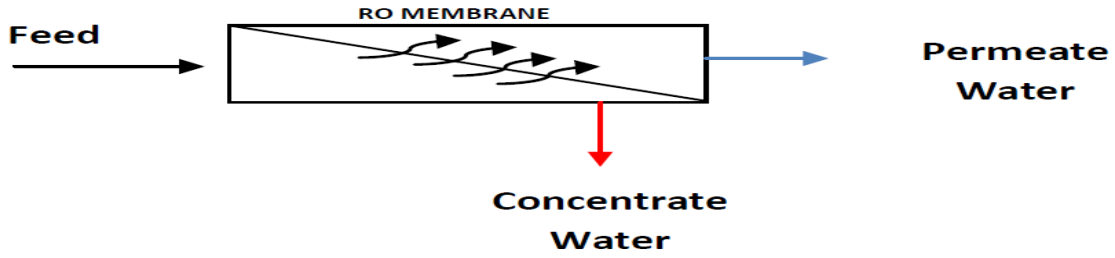


**Figure 7 Single stage RO**

In the double stage RO configuration, the concentrate from the first stage is used as the feed for the second stage, while the permeate from first stage is collected and combined with the product of the second stage. As the number of stages increase, the system recovery increases. Figure 8 shows a double stage system in which the concentrate of the first 2 vessels (first stage) is used as the feed for the third vessel (second stage).

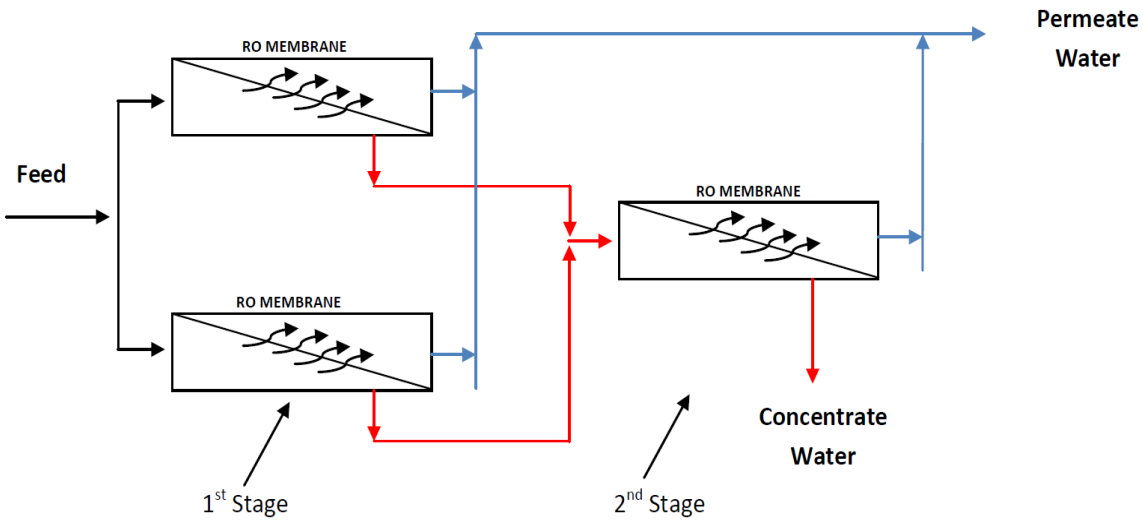


**Figure 8 Double stage RO**

In a single pass RO, the permeate only goes through one membrane. The pass can be thought of a stand-alone RO system. The product of the system is directly collected after the membrane and does not pass through another membrane. Figure 9 shows a schematic of the configuration.

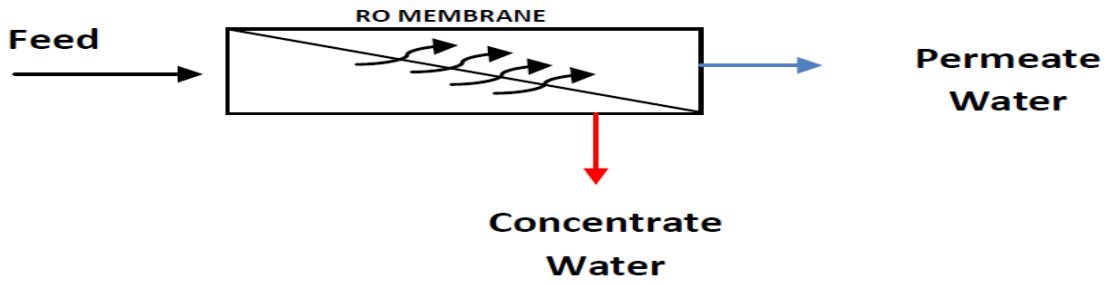


**Figure 9 Single pass RO**

In the double pass RO configuration, the product leaving the first pass is utilized as the feed for the second pass and hence resulting in a higher product quality because the product passes through two membranes. Figure 10 shows this configuration.

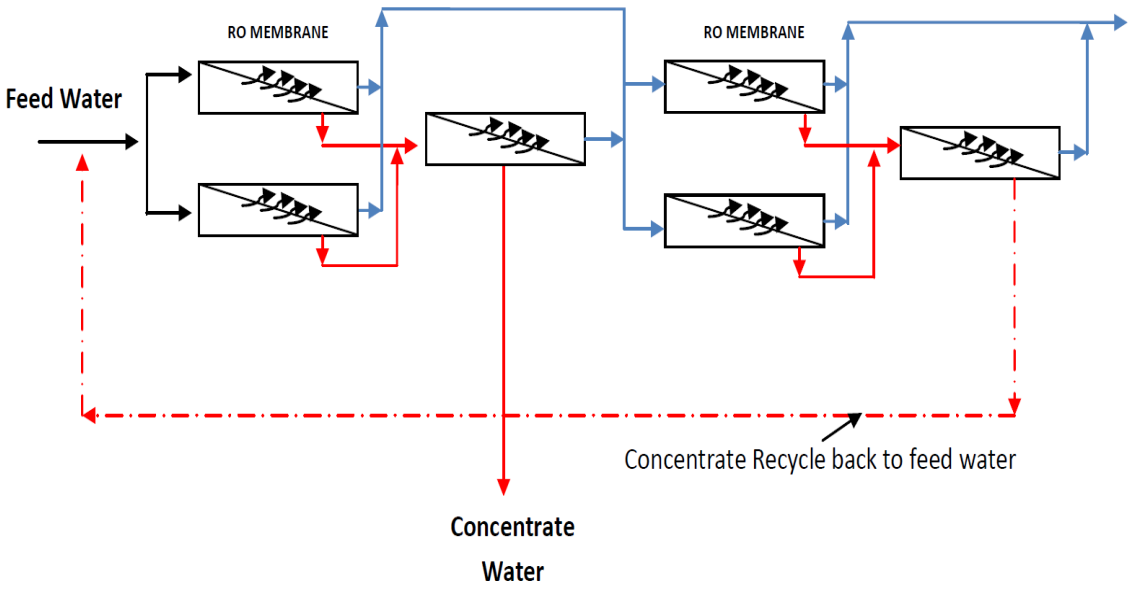


**Figure 10 Double pass RO**

RO with concentrate recirculation, which is one way to increase the system recovery, part of the concentrate that would have been rejected is recirculated. Figure 11 shows an RO system with concentrate recirculation [8].

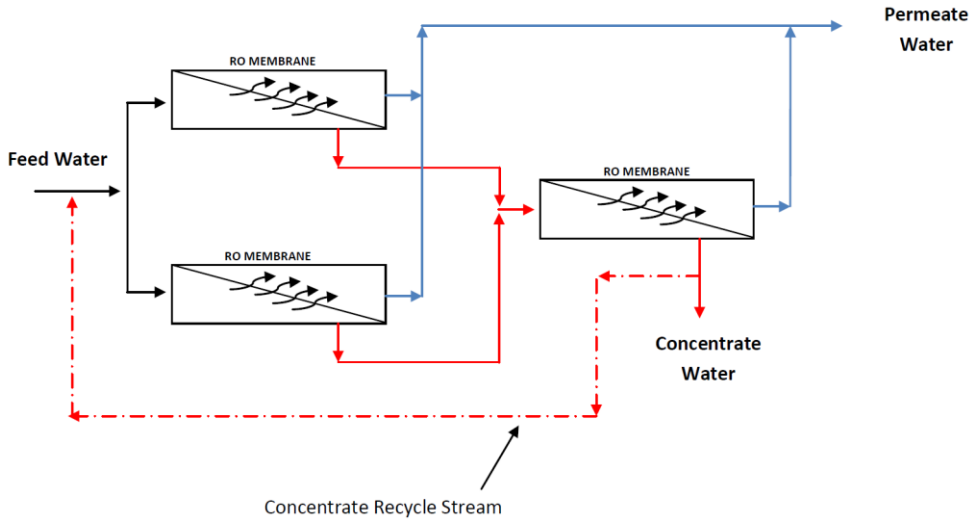


**Figure 11 RO with brine recirculation**

### 1.3.2 Forward (Direct) Osmosis

Forward osmosis is a membrane process that is osmotically driven. It uses the pressure gradient to drive water molecules from the feed side to the high concentration draw side. The feed side has a low osmotic pressure while the draw side has a high osmotic pressure [9].

The draw solution has a concentration higher than that of the feed water, causing the water to flow across the membrane into the concentrated solution. The selection of an efficient draw solution can, to a great extent, determine whether the FO process is feasible or not. The draw solution should have high solubility in water and low molecular weight to generate high osmotic pressure. It should also be non-toxic and chemically compatible with the membrane [10].

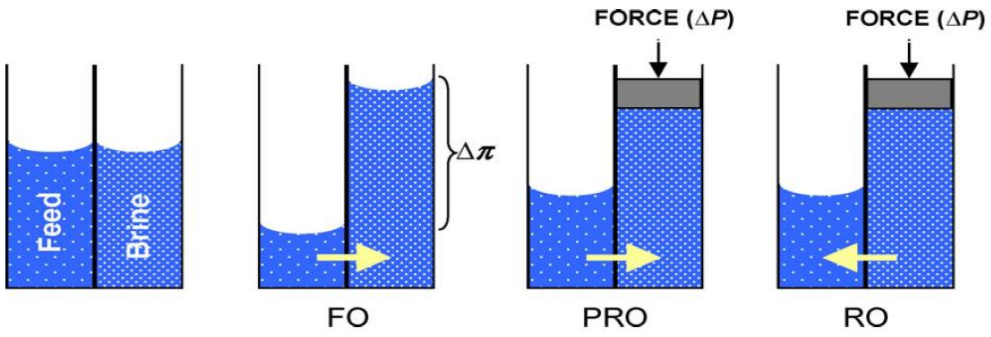


**Figure 12 Flow directions in FO, PRO, and RO. [11]**

PRO, although not a desalination technique, as represented in Figure 12 can be seen as an intermediate process between FO and RO. The applied hydraulic pressure is less than the osmotic pressure difference and hence the water flow direction is the natural osmosis direction.

Unlike reverse osmosis (RO), in which the applied pressure is the driving force, the osmotic pressure is the driving force used to transfer the water through the membrane. The pressure involved in the FO process is only that due to the flow resistance in the membrane module (a few bars).

Forward osmosis applications include wastewater treatment separation processes, food processing, seawater or brackish water desalination, electricity generation using pressure-retarded osmosis, and osmotic pumps used for drug release. Figure 13 shows the applications of FO.

It has several advantages over the pressure-driven processes such as reverse osmosis (RO) due to the very low hydraulic pressure required. These advantages include the following: lower energy consumption (the energy required for pumping is about 0.5 kWh/$m^3$), less

fouling, easier fouling removal, and higher water recovery (less brine), which is environmentally favorable.

After the water is drawn across the membrane, low-grade heat will be used to disrupt the solution to obtain freshwater, while the draw solution is used again to draw water. The draw solution used in the work of McCutcheon et al. is a solution of ammonium bicarbonate salt $NH_4HCO_3$ in water [10]. Figure 14 shows their novel ammonia-carbon dioxide FO process.

Freshwater can be later separated from the draw solution by moderate heating (about 60°C) causing the decomposition of ammonium bicarbonate into $NH_3$ and $CO_2$ gases, which are removed by low-temperature distillation (a distillation column). Waste heat can be used for the separation process.

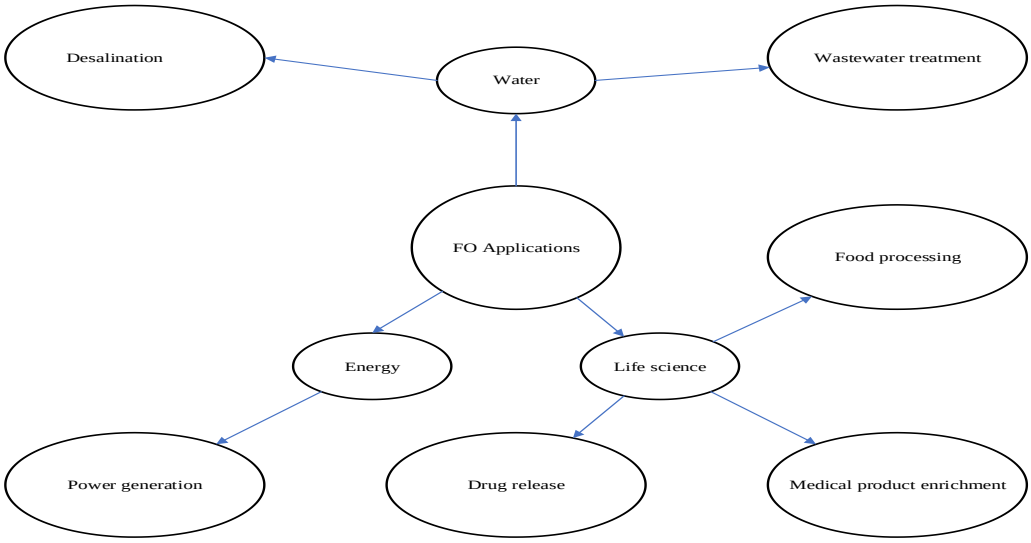


**Figure 13 Different FO applications**

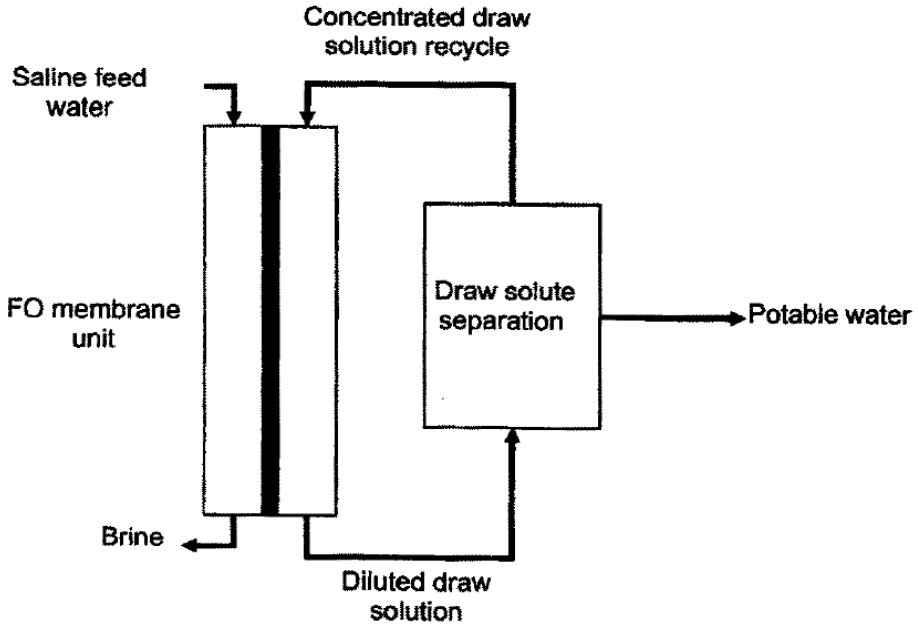


**Figure 14 $NH_3$-$CO_2$ FO process.[10]**

### 1.3.3 Nanofiltration

Nanofiltration is a membrane technology that is relatively new and is mostly used for water with low TDS (e.g., surface water and brackish water). Reverse osmosis, ultrafiltration, and microfiltration were introduced as three separation processes resulting from the development of a new process for manufacturing polymeric membranes. However, the shortcoming of these polymeric was the operation range of the three separation processes. This shortcoming was overcome with the development of nanofiltration in the late 1980s [12].

In addition to its main application of water treatment, nanofiltration can be used in many other applications in the food industries, chemical processes, wastewater treatment, paper manufacturing, and in textile factories. These applications of nanofiltration are not limited

to water-based solutions. Nanofiltration has been used for other types of applications and treat non-aqueous suspensions. For example, nanofiltration can be applied in petroleum refineries.

Examples of the work done in applying NF include the following: desalination (e.g., work of Wang et al. [13]), purification (e.g., work of Li et al. [14]), freshwater production (e.g., work of Wang et al. [15]), and wastewater treatment (e.g., work of Ratana et al. [16]).

The key difference between nanofiltration and reverse osmosis is in the type of salts they remove. Reverse osmosis removes monovalent salts, while a nanofiltration membrane lets them through while blocking divalent salts. Another difference is that nanofiltration requires a lower operation pressure than reverse osmosis, which means a lower cost of energy in the case of a NF system compared to a RO system.

## 1.4 Water Desalination Powered by Renewable Energy

The driving force for introducing and implementing renewable energies in desalination is the increase in the amount of freshwater required by mankind [17]. Using renewable energy to meet the energy requirements of desalination processes can be very helpful in remote areas and will decrease the negative environmental impact of conventional methods and make the water production process more sustainable. Renewable energy can be used directly by utilizing the produced heat or pressure as energy input to the desalination process or indirectly by utilizing the electricity generated from renewable energy for desalination. Both of the two aforementioned approaches require the use of energy storage to ensure a steady energy supply for the desalination process.

Desalination processes that can be integrated with solar energy include direct desalination processes, such as the solar still and HDH and indirect processes, such as MED, MSF, solar powered RO, and solar powered MD. Renewable energies that can be coupled with desalination plants include wind, solar thermal, photovoltaic, and geothermal.

Desalination based on renewable energy is becoming more economically attractive as the desalination cost is decreasing and so does the cost of renewable energy technologies, while the fossil fuel cost is increasing. Desalination based on renewable energy was less than 1% of the desalination capacity based on conventional fuels according to the EU estimates of 2008 [18]. The dominant form of desalination technology based on renewably energy is RO, which represents 62% followed by thermal MSF and MED. Solar photovoltaics are the dominant form of renewable source with a 43% share followed by solar thermal and wind energy.

Many attempts and experiments have been carried out on coupling solar energy with desalination systems. The suitability of a certain renewable energy source to a certain desalination process depends on the form of energy the source will provide and the requirements of the desalination process [19]. Based on this fact, several combinations of renewable energy sources and desalination technologies can be used. Some of those are shown in Figure 15 [20].

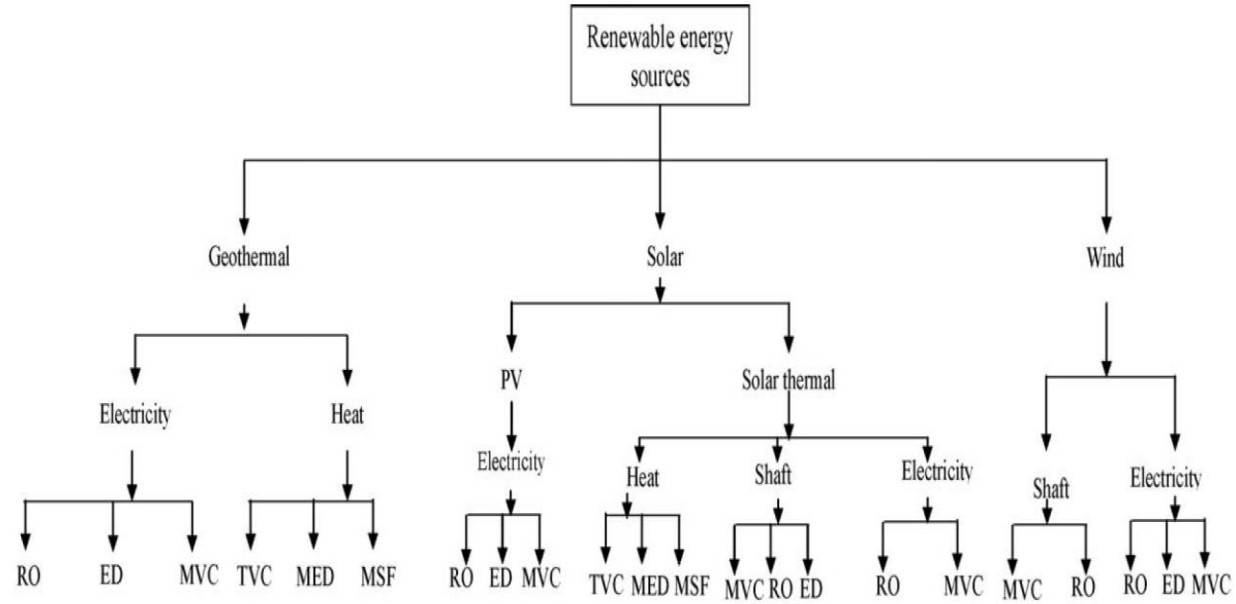


PV= Photovoltaic, RO= Reverse osmosis, ED= Electrodialysis, MVC= Mechanical vapor compression, MED= Multi effect distillation, MSF= Multi stage flash distillation, TVC= Thermal vapor compression

**Figure 15 Different renewable energy sources and their possible integrations with different desalination technologies**

## 1.5 Significance of the Work

This work derives its significance from the importance and seriousness of the problem it addresses, i.e., water scarcity worldwide. The Middle East and North Africa region is one of the most severely affected regions in the world by this problem. As water desalination is known to be a key solution to address water scarcity, it is essential that all possible technologies and membrane technologies are investigated.

The outcome of this work will provide decision makers a full insight on the NF/FO/RO hybrid system and the possibility of coupling it with renewable energy resources and the feasibility of the configuration for Saudi Arabian conditions.

## 1.6 Motivation of the Work

The changing climate and unsustainable human activities have exacerbated the severity of the water crisis due to the very limited renewable water resources in many places around the world including Saudi Arabia. Considering that one of the main disadvantages of currently used water desalination technologies is the high consumption of power, the use of the different types of renewable energies shows great promise to address this issue and makes systems run completely or partially by renewable energies increasingly attractive.

Saudi Arabia and other countries affected by the water scarcity problem have an abundance of different renewable energy sources. For instance, Saudi Arabia lies in the sun belt which means it receives a large amount of solar energy around the year. This and other renewables, such as wind, can provide all or some of the energy required to produce the

freshwater required for human needs and other uses. This work is expected to help tackle the water shortage problem in Saudi Arabia.

The current work aims at investigating the possible options of coupling membrane water desalination systems with renewable energy sources in Saudi Arabia. It also aims to provide a setup and operation scenarios that are best in terms of the amount of water produced and energy consumed (Economy).

## 1.7 Objectives of the Work

The main objective of this work is to investigate the performance of a solar powered hybrid NF/FO/RO desalination system and determine its feasibility and implementation possibilities under the weather conditions of Saudi Arabia. The specific work objectives are the following:

- Develop a model for determining the energy requirements for the proposed NF/FO/RO system and the related processes.
- Investigate different coupling options between the NF/FO/RO system and solar and wind energies. Coupling options of interest here are the solar, wind, and solar/wind, considering electricity storage as a part of the system.
- Study different operation scenarios including different operation periods and the fraction of energy from each renewable energy source based on the time of the year and availability.
- Compare the studied coupling options and operation scenarios to determine the best option for system coupling with renewable energy in terms of freshwater productivity and cost.

## 1.8 Research Methodology

The objectives of the proposed work will be achieved through the following steps, which are briefly described in this section: 1) Literature review, 2) Modeling and validation of the hybrid NF/FO/RO system using EES, and 3) Use of HOMER software to couple the system with renewable energy sources.

### 1.8.1 Background and literature review study

A background summary was written about the water and water related challenges including different water desalination technologies covering the status of current research focusing on the technologies comprising hybrid systems. A number of previous studies focusing on integration with renewable energies and different possible integration options were also summarized.

### 1.8.2 Model NF/FO/RO hybrid system

Engineering Equation Solver was used in this part to simulate the performance of the hybrid membrane system and validate the results against those of previous work. The results were obtained for different feed water salinities and presented.

### 1.8.3 HOMER Analysis

HOMER software was used in this part of the work to simulate the performance of the system under different coupling and operation scenarios with solar and wing energies. This was followed by determining the best option and cost analysis study.

# CHAPTER 2

# LITERATURE REVIEW

## 2.1 Water problem and the need for desalination

Freshwater is the one of the most important requirements of all civilizations. In modern times, however, freshwater resources are becoming more and more scarce. This can be witnessed in some parts of the world as the severity of this issue varies depending on many variables.

The increasing water scarcity is attributed to the increasing human population is placing on available water resources and urbanization.

Of the 1.4 billion $m^3$ of water on earth only 2.5% is fresh water that can be used directly for all purposes such as for drinking. More interestingly, about 70% of this 2.5% is contained in ice caps and glaciers and hence not accessible at a reasonable cost. Of the remaining 30%, 97% is groundwater and 3% is surface water in rivers, lakes and the likes. Fig. 16 shows a detailed summary of the available water on earth. Table 1 shows the amount of freshwater withdrawn in several countries in the past compared to the renewable water resources. According to this table, Saudi Arabia has the smallest quantity of available renewable water resources while raking 3$^{rd}$ highest in water withdrawals in among the listed countries. This alone is an indication of the importance of desalination in this region.

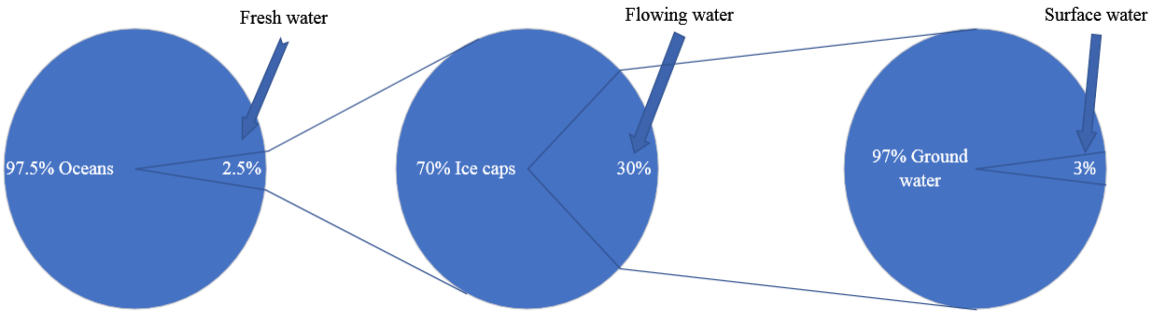


**Figure 16 Breakdown of water available on the planet**

**Table 1 Renewable freshwater resources and withdrawal for some countries** [21]

| Country | Year | Renewable water resources | | Water withdrawal |
|---|---|---|---|---|
| | | Total | Per inhabitant | |
| | | (bn $m^3$) | ($m^3$) | ($m^3$) |
| Australia | 2002 | 492 | 25034 | 1218 |
| Egypt | 2002 | 57 | 786 | 937 |
| Germany | 2002 | 154 | 1873 | 473 |
| Norway | 2002 | 382 | 84178 | 483 |
| Saudi Arabia | 2007 | 2 | 97 | 959 |
| Spain | 2002 | 112 | 2703 | 864 |
| United States | 2007 | 3069 | 9943 | 1550 |

These numbers leave the human population with almost negligible amount of freshwater compared to the total amount of available water. This leads people to focus on converting saline and brackish water into freshwater to compensate the deficit.

This automatically brings up desalination as a solution to this problem. Desalination can be classified into thermal desalination and membrane desalination. As all the techniques used in the current work are membrane-based techniques the following literature review will focus on them.

## 2.2 Membrane desalination

The following sections will briefly discuss some of the work done on membrane systems which are considered for this work. Each of the sections will be dedicated to one system to provide information on certain aspects related to that system.

### 2.2.1 Reverse osmosis

Reverse osmosis process utilizes a semi permeable membrane that only lets water molecules pass through and blocks almost all salt particles. This is done by applying pressure to reverse the action of the osmosis phenomenon. Figure 17 illustrates the operation concept of RO membranes [22].

A typical RO plant comprises four major processes performed by the components described earlier. Studies of such plants can be found in the work of Ayyash et al. [23] and Baig and Al Kutbi [24]. Ayyash et al. discussed the performance of a 33.8 MGD SWRO plant in Medina and Yanbu, Saudi Arabia and how the properties of the produced water were different from the anticipated and the investigation that followed and its results. Baig

and Al Kutbi described the design aspects of a 20 MIGD SWRO plant in Jubail, Saudi Arabia. The basic design criteria, pilot plant studies, pretreatment media filters, water supply system, and RO desalination units were among the aspects covered in their study.

An economic and technical investigation of a proposed medium-size RO plant was detailed in a study by Al-Karaghouli and Kazmerski [25]. The analysis was done using DEEP software of the IAEA. The quality of the produced water and its cost, effect of electricity price on water cost, seawater salinity effect on the cost of freshwater, and the effect of interest rate and seawater temperature were all studied and results were presented.

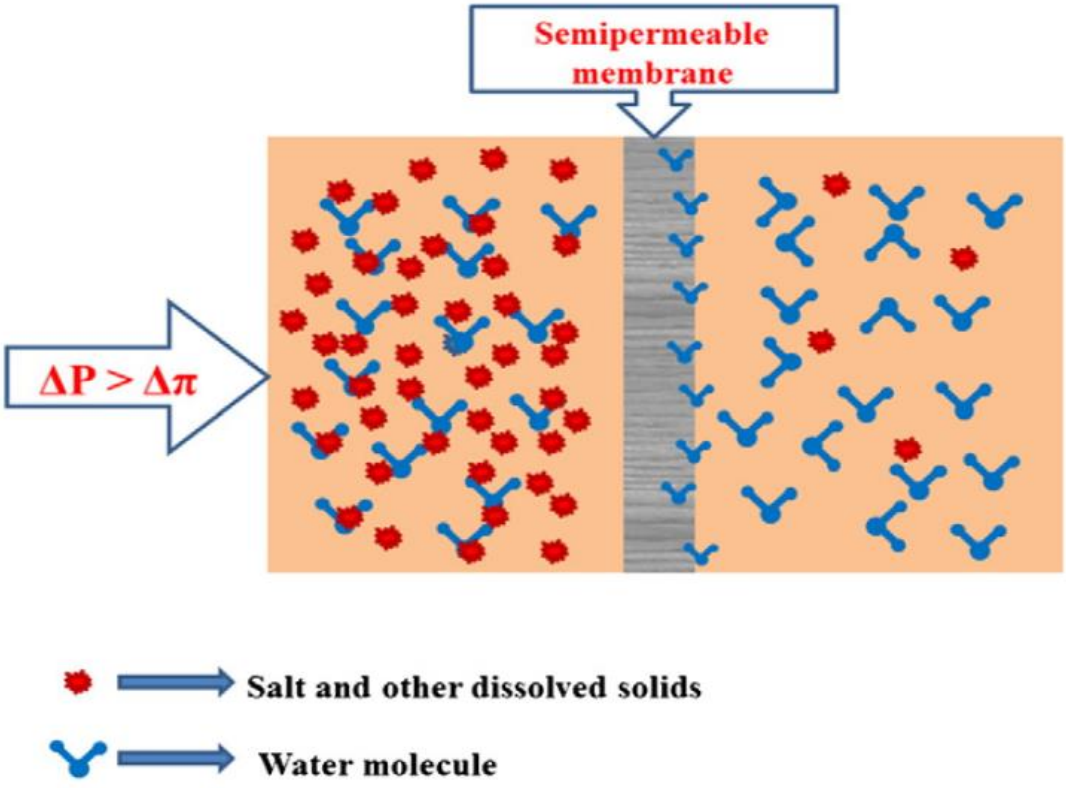


**Figure 17 RO membrane working mechanism**

Reverse osmosis process is known to be associated with problems such as scaling, brine disposal, and boron removal. Scaling is the precipitation of salts on the membrane surface

when a supersaturation level of salts is reached. Hasson et al. [26] did investigate the effect of $CaSO_4$ scaling on RO membranes at different recovery ratios and found that it affects the productivity of the membrane. This problem can be addressed by the use of anti-scaling agents, which increases the threshold for supersaturation of salts and hence scale formation. Examples of anti-scaling agents include organic polymers, phosphates, and surface-active reagents [27].

Meeting the WHO requirements on the maximum boron content of 0.5 mg/L in drinking water makes removal of boron of high importance in the RO process. Because RO itself cannot remove boron effectively, a RO plant consists of two passes or more. When seawater passes through the first high-pressure membrane the pH is not adjusted, while in the second one a low-pressure brackish water membrane is used. This arrangement of passes which includes elevating the pH in the latter one, insures a higher boron removal effectiveness [28].

Discharge into water bodies, evaporation ponds, and well injection are examples of the methods currently in use for the disposal of the brine from a desalination system (reject or concentrate). As the brine has a higher salinity than the body it is dumped in and contain anti-scalants, anti-foulants, and corrosive materials, brine poses a potential environmental threat [29].

### 2.2.2 Forward osmosis

McCutcheon et al. [30] presented a novel FO desalination process that used ammonium bicarbonate as a draw solution and a polymeric membrane. The driving pressure across the membrane was generated by osmotic pressure difference across the membrane. The extraction of freshwater was achieved by moderately heating the ammonium bicarbonate solution. It was reported that a relatively high salt rejection and high product flux can be obtained from a laboratory-scale unit and that RO membranes give relatively low water flux when used for the FO process.

Another study on the ammonia-carbon dioxide system is that of McGinnis and Elimelech [31]. They used the chemical energy process software HYSYS to predict the energy requirements of the FO system including thermal and electrical energy requirements. An equivalent of electrical energy was also calculated. The results showed that the energy savings by using FO compared to conventional desalination technologies fall in the range of 72% to 85%.

A pilot FO plant was tested by McGinnis et al. [32] that treated water of salinity in the range of 73,000 mg/L. The plant featured pretreatment process including chemical softening and carbon cartridge filtration among others. The study results showed that the plant has a 64% recovery ratio, 2.6 L/$m^2$-h water flux, 180,000 mg/L TDS brine, and 300 mg/L product water.

The effect of the concentration of the feed and draw solutions on the FO process was investigated in a study by McCutcheon et al. [33]. Ammonia-carbon dioxide system was used as the draw solution. The experimental work was done in a crossflow, flat-sheet

filtration cell in which commercial FO membranes were used. Due to the internal concentration polarization, the obtained water fluxes were much less than expected in which the draw solution was found to play a major role.

Lutchmiah et al. [34] reviewed the use of FO in wastewater treatment as a way to help alleviate the drinking water scarcity problem by using treated wastewater in industrial applications. Membrane materials, effective draw solutions, membrane fouling, fouling effects, and fouling cleaning energy aspects were among the covered aspects of membranes use in wastewater treatment.

### 2.2.3 Nanofiltration

The use of a loose NF membrane for the purpose of arsenic removal from drinking water was investigated by Vrijenhoek and Waypa [35]. Arsenic removal efficiency of the NF membrane with respect to changes in pH, the arsenic concentration of the feed, and background presence was experimentally tested. 60-90% of arsenic was removed for multiple synthetic waters with varying arsenic concentrations. The percent removal was enhanced at higher pH and in the presence of 0.01 M NaCl.

Ratana et al. [16] experimentally evaluated the performance of three different commercial NF membranes (NTR-729HF, ES20 and LES90); the first of which was neutral and the other two were negatively charged. The performance was evaluated in terms of permeate flux and salt rejection. Three feed solutions were used in the experiments; RO-deionized water, sodium chloride aqueous solution, and dye aqueous solution.

Another experimental NF membrane separation work was reported by Li et al. [14]. NTR7450 membrane was used to separate L-glutamine from fermentation broth.

Parameters whose effect on the membrane's performance included transmembrane pressure, pH, and concentration of broth. A single amino acid solution was used in the experiments. The effect of of Glu and Gln, Gln concentration of the fermentation broth, ionic composition of the Glu and Gln solution, and glucose in broth of the NF membrane were investigated.

A dual NF-NF process for seawater desalination was developed by Vuong [36]. The reported power consumption was 20-30% lower for one-stage RO. A plant that was based on this concept was constructed in Long Beach and produced 1135 $m^3$ of fresh water as reported by Adham et al. [37].

Zhou et al. [38] investigated the current status of efforts to integrate the NF process with other desalination technologies (membrane and non-membrane based) for the purpose of reducing the cost of water desalination. Various integrations with RO, FO, ED, MSF, MED, MD, and IX were reviewed.

### 2.2.4 Hybrid membrane systems

Shaffer et al. [39] proposed an integrated RO and FO process for seawater desalination for agricultural applications. The main focus of their work was the stringent agricultural irrigation water requirements for boron and chloride. The process was modeled and the obtained results showed that it can meet the boron and chloride requirements. It was also shown that the energy consumption was also less than that of a conventional two-pass RO process.

Choi et al. [40] investigated the integration of FO and RO processes, considered concentration polarization in both processes and used a laboratory-scale FO system for

further calculations. The water flux was calculated and compared to that from the experimental setup under different operational conditions. It was obvious that the integration of FO and RO processes results in higher flux than the that of the FO process alone under some conditions.

Another hybrid membrane system was described by Yangali-Quintanilla et al. [41] that featured an FO system integrated with a low pressure RO (LPRO) one. The system was implemented for indirect desalination and the results showed that it consumes about 50% less energy compared to a high pressure SWRO while producing water of good quality. The experimental setup was tested over 14-day period and FO fouling was not a major issue during that period. 28% drop in the flux was observed after 10 days of operation and cleaning the FO membrane recovered 98.8% of the initial flux.

A novel FO-NF seawater desalination process was proposed by Tan and Ng [42] and was investigated on a laboratory-scale test cells using seven different draw solutions. Product water flux of 10 $L/m^2$ was achieved for both membrane processes. The product from this system has a TDS of 113.6 mg/L and $Na_2SO_4$ and $MgSO_4$ were proposed as the most suitable for the hybrid process.

Altaee et al. [43] did a comparison of an FO-RO process to a RO process. The FO-RO has high efficiency and can be applied to a range of ionic solution treatments and hence was meant to be used for draw solution regeneration. The comparison was done using a pre-developed software and the results showed that while the power consumption of the FO-RO process was higher than that of the RO process the difference was insignificant for a

0.65 mol $MgCl_2$ FO-RO. The results also showed that the difference decreased with higher water salinities.

A hybrid desalination process that comprised FO, ED, and RO systems was introduced by Bitaw et al. [44]. The proposed system utilized an FO element upstream of an ED-RO system. Sodium chloride was among several draw solutions selected based on their conductivity and assessed for use in the system. Parameters considered in this study were energy consumption, unit process sizes, and their production cost. Ammonium chloride was determined to be the optimum draw solution with fresh water cost of 0.514 USD/$m^3$ and achieving the goal of decreasing the energy consumption.

## 2.3 Renewable energy powered membrane desalination systems

One of the main factors believed to shape and determine the future of membrane desalination processes is the use of renewable energies to power those systems. This will minimize the effect of two of the present limitations of the membrane-based desalination systems which are the significant specific energy consumption and the environmental impact, e.g., production of GHG.

### 2.3.1 Reverse osmosis

Conventional desalination methods rely on fossil fuels. Powering those using renewable energy can break that dependence and reduce the operation cost substantially, producing a lower environmental effect. Its reported that PV-powered RO can produce water at a cost as low as \$2-3/$m^3$ [45]. Figure 18 shows a simplified PV-powered RO with a storage system.

Due to the fact that PV modules were the first commercialized solar energy technology, it is frequent that a solar powered RO system is comprised of RO membranes and an array of PV modules. The DC current generated by the PV modules is used to drive the pumps that provide the hydrostatic pressure needed for the RO process. Because of the low conversion efficiency and high price of the PV modules, many studies were dedicated to determining the economic feasibility of RO-PV system.

RO-PV have been used for both brackish water and seawater desalination. The components of a typical RO-PV system include: PV modules, water extraction unit (feed pump), pretreatment unit, high pressure pump, RO membranes, AC/DC inverter, and electricity storage (batteries).

The modules used can be both mono or multi-crystalline silicon modules. They can be fixed or adjustable (tracking). The feed pumps are used to deliver the seawater or groundwater from wells to the RO pretreatment stage. The high-pressure pump is used to apply pressure that is higher than the osmotic pressure difference on the feed water. Normally positive displacement pumps are used because of their higher efficiency compared to centrifugal pumps. The inverters are used in case the system implemented AC pumps and motors. RO-PV systems that run DC pumps are expected to have higher energy efficiencies because DC motors have less energy losses. The batteries are used for two reasons: to balance the energy output of the PV modules during the day or to extend operation hours beyond daylight hours.

Helal et al. [46], studied the economic feasibility of a 20 $m^3$/d RO plant run by three power alternatives: PV + diesel generator, diesel generator alone, and PV alone. Figure 19 shows the simplified plant.

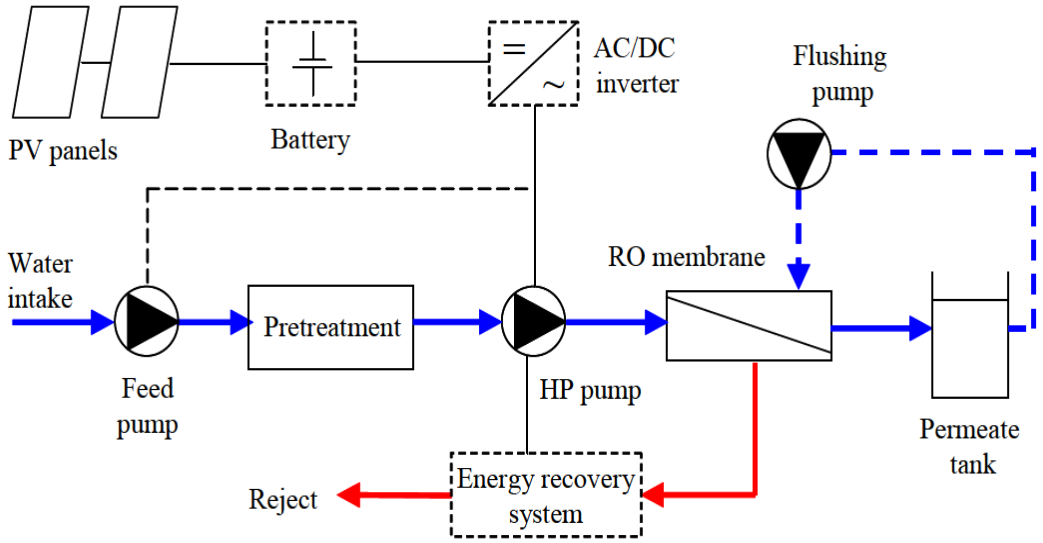


**Figure 18 Simplified RO-PV system** [45]

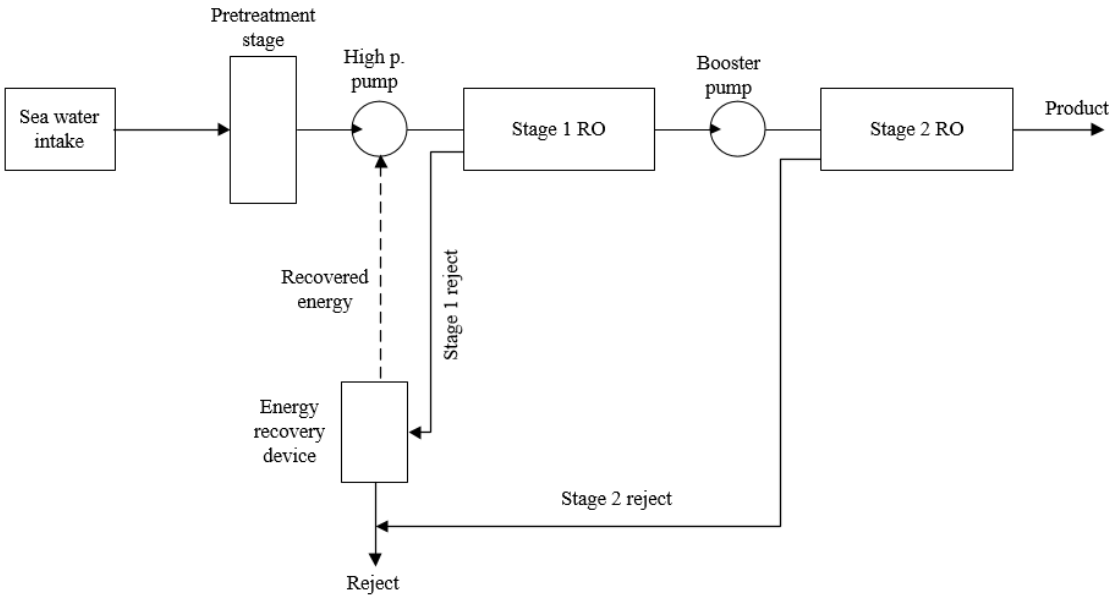


**Figure 19 Simplified double stage RO plant flow sheet** [46]

Mohamed and Papadakis [47] proposed a desalination unit comprising a RO system that was being powered by a hybrid wind-PV renewable energy integration. Energy recovery was also implemented in the proposed system with the RO process. Then the operation simulations were conducted and water cost and energy saving percentage were calculated when using a pressure-exchanger energy recovery device.

Another novel stand-alone RO desalination plant that was powered by PV and pressure retarded osmosis (PRO) was studied by Wei He et al. [48] Two operational schemes based on which of the two considered power sources is used were investigated and their feasibility was studied. The work done included thermodynamic feasibility analysis, numerical feasibility analysis, determination of operational windows, study the effect of some parameters on operational windows, and a case study was done for Perth, Australia.

They modeled the PV system to calculate the power output, calculated carbon dioxide emissions, estimated the costs and concluded that the selection of the optimum design depends on the primary energy cost and the cost of the PV panels.

Joyce et al. [49], described a small RO-PV system that can be used to produce freshwater in rural areas. The system was assembled, tested and the yearly water production was estimated. The cost of the produced water was also estimated. Figure 20 shows a schematic of the system.

The performance of the system when coupled with 2 and 3 30Wp PV modules was monitored. The obtained pressure in the two cases was 3.3 and 4.2 bar, respectively. The water flow rate varied between 140-200 L/h depending on the PV current.

Table 2 summarizes some of the technical specifications of some PV-powered RO systems at different locations around the world.

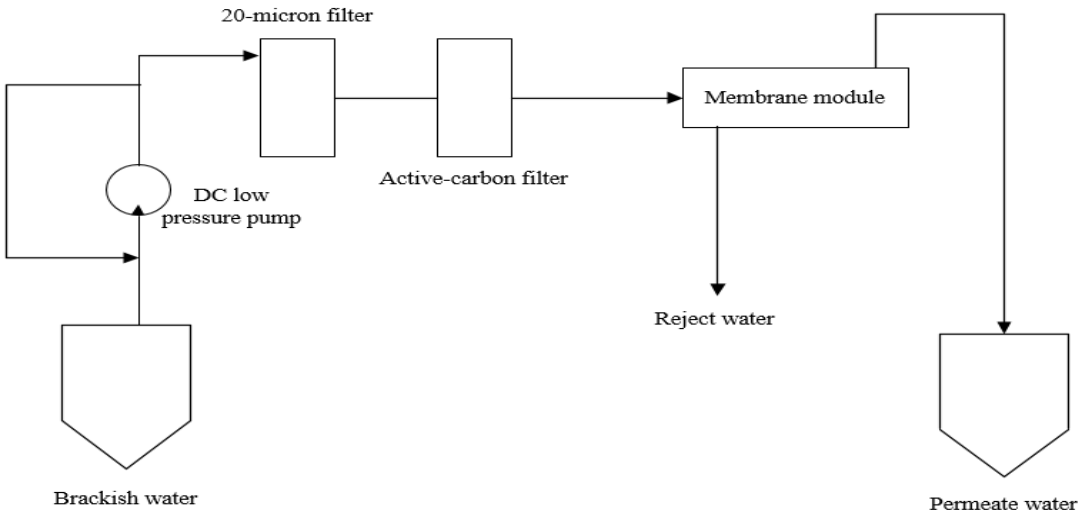


**Figure 20 A small RO-PV system for rural areas** [49]

**Table 2 Some PV-powered RO systems**

| Location | Year | Capacity ($kW_p$) | Battery | Pump drive | Production ($m^3/d$) | Water cost ($USD/m^3$) |
|---|---|---|---|---|---|---|
| Riyadh [50] | 1994 | 10.08 | Yes | AC | 5.7 | 9.6 |
| Qatar village, JOR [51] | 2000 | 32 | Yes | AC | 45 | 9.6 |
| Athens, GRC [52] | 2006 | 0.85 | No | DC | 0.35 | 9.8 |
| Hammam Lif, TUN [53] | 2003 | 0.59 | No | DC | 0.05 | 11.6 |
| Abu Dhabi, UAE [46] | 2008 | 11.25 | No | AC | 20 | 7.3 |
| Pine Hill, AUS [54] | 2008 | 0.6 | Yes | DC | 1.1 | 3.7 |
| Denver, ITN, USA [55] | 2003 | 0.54 | No | DC | 1.5 | 6.5 |

### 2.3.2 Forward osmosis

Khaydarov and Khaydarov [56] constructed a 1 $m^3/h$ seawater desalination pilot FO device. The device was powered by 12V, 500W solar batteries to power the pumps. It also featured solar thermal exchangers and a pretreatment unit. The salinity of the produced water after post-treatment was 50 mg/L, while salinity of the saline water was 17 g/L. The device can be used for treatment of water with salinities up to 40 g/L.

Schrier [57] proposed that FO to be used for the production of fuel-grade ethanol instead of the conventional costly distillation process. Solar evaporation was utilized for the regeneration of the aqueous brine which is used as a draw solution. Ethanol solutions of 95%, 50%, and 30% for cooking and HCCI were focused upon. The effect of meteorological variables on the draw solution regeneration process was analyzed. The use of a subsequent distillation process after the FO process is recommended.

Another study that focused on the renewable energy-powered FO was the modeling of a solar FO pilot plant by Khayet et al. [58]. The response surface methodology was implemented in the modeling. Powering by both photovoltaics and solar thermal was optimized. Parameters considered in the study include permeate flux and specific performance index to study the effect of feed flow rate, permeate flow rate, and temperature. Experiments were conducted to confirm the optimum parameters from the simulations which included a specific performance index ranging between 25.79 and 0.62 L/g kWh at 0.83 L/min feed flow rate, 0.31 L/min draw solution flow rate, and 32.65°C temperature.

FO integration with solar energy is also used in a pilot seawater desalination plant that is to be constructed in the United Arab Emirates by Trevi Systems of Petaluma, California. The system will be using solar thermal energy for draw solution regeneration. The plant capacity will be 1760 cubic feet per day [59].

Monjezi et al. [60], studied the coupling of an FO with a solar pond and using the energy from it to regenerate the draw solution which was chosen to be dimethyl ether. A 10000 $m^2$ solar pond in Chabahar, Iran was determined to be able to drive a 5210 $m^3$ FO process in the first two years of operation. The cost of the freshwater from this process was 0.46 $kWh/m^3$.

### 2.3.3 Hybrid membrane systems

Iaquaniello et al. [61] proposed and studied a system that integrates concentrating solar power (CSP) with MED process and an RO process. The low temperature exhaust from a back-pressure steam turbine (BPST) and the electricity from the turbine was used to power the RO process. A gas turbine was also used as a backup to generate electricity for the RO process. The most effective contribution of the solar thermal and electricity in powering the system was determined and an economic analysis of the system followed that.

Hoyer et al. [62] proposed and experimentally investigated a hybrid FO process with thermal draw solution regeneration that can be done by solar heat or waste heat. The draw solution was a surfactant water emulsion. 12 different surfactants were experimented and it was found that L31 surfactant gives the optimum performance. It has high water affinity in FO and requires low regeneration temperatures of 50°C. In order to produce drinking

water, further purification is needed and NF was determined to be the most suitable method.

Mabrouk and Fath [63], [64] experimentally evaluated a hybrid NF-MSF pilot plant powered by renewable energy. The MSF has MSF-DBM configuration. The NF process enables the MSF to operate at higher TBT. The system was tested under TBT = 100°C giving a GOR of 15. The results of the experiments were compared to those of a simulation resulting in good agreement. In the other work, the TBT was raised to 130°C and a techno-economic study of the system was conducted. The work studied NF integration with MSF-BR and MSF-DM configurations. The analysis results of NF-MFS-BR showed an increase of 19% in water production while cost increased by 5.4% compared to conventional MSF at TBT = 110°C. On the other hand, the analysis of NF-MSF-DM showed that the levelized water cost was 14% lower than that of a conventional MSF at TBT = 110°C at the oil price at that time.

A performance analysis of a tri-hybrid NF/RO/MSF pilot plant for seawater desalination was reported by Hamed et al. [65]. They presented operational performance of the pilot plant and established optimum operating conditions. The recovery ratio of the NF process was 64%, while that of the SWRO was 47%. The MSF was operated at TBT up to 130°C due to the low calcium and sulphate ions concentration of its feed resulting in a recovery ratio of 69%.

## 2.4 Literature review summary

From the variety of systems and studies covered in the literature review its clear that there is a need for a system that mitigates the need for extensive pretreatment of brackish water before membrane desalination systems and lessens the effects of fouling and scaling. It is also evident that the integration of such a system with renewable energy sources can be an attractive alternative to using conventional fuels and hence reducing gasses emissions and protecting the environment.

The hybrid membrane system considered in this study will address these points and also provide an in-depth look into the possibilities of coupling with renewable energy sources.

# CHAPTER 3

# System Modeling

## 3.1 Problem formulation

The following sections of this chapter will describe the system-modeling steps in detail and their expected outcome. They will be concerned with the system selection, modeling of the hybrid system, the integration with the renewable energy sources, and modeling using HOMER software. A brief description of the software used and a discussion of the cost analysis of the overall desalination system are also included.

### 3.1.1 System selection criteria

The system used in this study was selected based on the higher recovery rates without the need of an intensive chemical pretreatment. An NF membrane with a loose structure is used for pretreatment and provides the first of two product streams. The intermediate FO membrane was chosen for its many advantages including low scale fouling propensity, lower power consumption, high recovery rates, and the controllability of it by adjusting the draw solution concentration.

### 3.1.2 System description

The system consists of three membrane sub-systems. The feed brackish water is fed to the NF membrane for the removal of most of the divalent ions and some monovalent ions and producing freshwater that can be used directly or mixed with the second product stream

from the RO membrane. The NF product water is considered to be low to average salinity. The NF membrane also serves as a pretreatment stage for the rest of the system. The brine (concentrate) from the NF membrane is fed to the intermediate FO process for further freshwater extraction and utilizing its low power consumption and high recovery rate among other advantages. The freshwater passes across the FO membrane driven by the osmotic pressure generated by the draw solution resulting in dilution of the draw solution itself. No high-pressure pump is needed here, unlike in the RO process. The diluted draw solution then leaves the FO process to the BWRO process where freshwater is extracted and the draw solution will be regenerated. Figure 21 shows a schematic of the system.

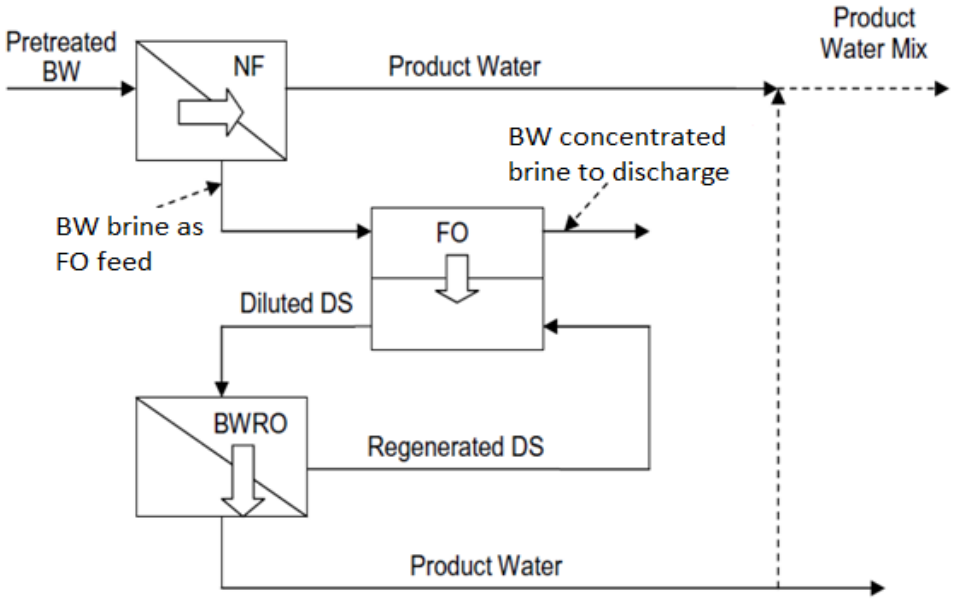


**Figure 21 The tri-hybrid NF-FO-RO system**

### 3.1.3 Mathematical model

The modeling of the proposed system will simulate its performance by focusing on three main parameters; (i) the system capacity or amount of freshwater produced, (ii) the quality

of salt concentration of the produced freshwater, and (iii) the specific energy consumption of the system.

The effect of some parameters such as the feed water properties, the concentration of the draw solution used in the FO membranes, and the recovery ratio on the above-mentioned performance parameters and the overall system performance is also investigated using the developed model. The following sections list and briefly discuss the equations and correlations used to model each of the three processes of the system.

## Modeling of the NF and RO systems

The nanofiltration process is the first of the three processes in the system. It generates two water streams that make up the total product of the system. Pretreated brackish water is fed to it and the resulting brine will be fed to the next FO process.

The RO is the final stage of the system. It is used to produce more fresh water and regenerate the draw solution for reuse. This is the most energy intensive of the three processes because of the high pressure that must be applied for the water to flow across the membrane in the opposite direction of the osmosis phenomenon.

The water flux of the NF, $J_w$, can be calculated from Eq. 1.

$$J_w = A_w\,(\Delta P - \Delta\pi) \qquad (1)$$

where, $A_w$ is the water permeability coefficient of the membrane, $\Delta P$ is the hydraulic pressure difference across the membrane, and $\Delta\pi$ is the osmotic pressure difference between the feed water side and the freshwater side.

The salt flux of the NF, $J_s$, can be calculated from Eq. 2.

$$J_s = B\,(C_f - C_{prod}) \tag{2}$$

where, $B$ is the salt permeability coefficient, $C_f$ is the feed concentration, and $C_p$ is the permeate water concentration.

The permeability coefficient can be calculated using Eq. 3.

$$B = \frac{(1 - R_j) * J_w}{R_j} \tag{3}$$

where, $R_j$ is the rejection rate of the membrane.

The specific power consumption can be calculated from Eq. 4.

$$E_s = \frac{P_f}{\eta * RR} \tag{4}$$

where, $P_f$ is the feed pressure, $\eta$ is the pump efficiency, and $RR$ is the recovery rate.

Generally, the recovery rate is the ratio of the permeate to the feed of a membrane system, described by Eq. 5.

$$RR = \frac{Q_{prod}}{Q_f} \tag{5}$$

The permeate concentration can be calculated using Eq. 6.

$$C_{prod} = B * C_{fc} * CP * R_j * \frac{A_m}{Q_{prod}} \tag{6}$$

where, $C_{fc}$ is the average concentration of the feed, CP is the concentration polarization, and $A_m$ is the effective membrane area.

## Modeling of the FO system

The FO utilizes the osmosis phenomenon to produce freshwater. A high concentration draw solution is used to generate the driving force for the freshwater to flow across the membrane. The higher the draw solution concentration, the higher the water flux. Thus, high pumping energy or high pressure are not required.

The feed of this process is the reject coming out of the NF process. This feed flows on one side of the membrane while the draw solution flows on the other side. The following equations describe the process.

The permeate flux, $J_{wFO}$, can be calculated from Eq. 7.

$$J_{wFO} = A_w\,(\Delta\pi) \tag{7}$$

As the process relies on the osmotic pressure difference, the hydraulic pressure term does not appear in the Equation.

The specific power consumption, $E_{sFO}$, can be calculated using Eq. 8.

$$E_{sFO} = \frac{P_f Q_{f-in} + P_D Q_{D-in}}{36 * \eta * Q_{prod}} \tag{8}$$

where, $P_f$ $and$ $Q_{f-in}$ are the pressure and the flowrate of the feed and $P_D$ $and$ $Q_{D-in}$ are the pressure and the flowrate of the draw solution.

Permeate concentration expression is similar to that used for the NF and RO membranes.

For the whole system, the total recovery ratio is calculated using Eq. 9.

$$Ret = \frac{Q_{pNF} + Q_{pRO}}{Q_f} \quad (9)$$

where, $Q_{pNF}$ and $Q_{pRO}$ are the permeate flow rates of the NF and RO systems, respectively.

For best energy consumption in the FO process, it is customary that the flow rates of the feed and the draw solution are set to be equal.

$$Q_{f-in} = Q_{D-in} \quad (10)$$

## 3.2 Software used

Engineering Equations Solver (EES) of f-chart software was used for mathematical modeling of the NF-FO-RO system. The program provides the ability to solve thousands of coupled non-linear algebraic equations. It also features a highly accurate database containing thermodynamic and transport properties. Hundreds of substances can be found in the properties library. It can also perform optimization, uncertainty analysis, check unit consistency, and produce high quality plots [66].

The Hybrid Optimization of Multiple Energy Resources (HOMER) of HOMER Energy LLC was used for the purpose of simulating the scenarios of coupling the desalination system with renewable energy resources. HOMER has the following three main powerful tools; Simulation, optimization, and sensitivity analysis. Simulation is the core of HOMER software. It can simulate thousands of possible systems depending on how the problem is formulated. HOMER optimization sorts the possible systems according to a user-specified optimization variable. HOMER optimizer uses a proprietary derivative-free algorithm that was built especially for this application. HOMER can also study the impact of a certain variable to help understand how it affects the optimal system [67].

## 3.3 Cost analysis

The following sections will detail the cost components, the assumptions used in the calculations, and the obtained results. The fixed and operating and maintenance costs will be detailed, assumptions will be listed, and results will be presented.

**Assumptions**

The assumptions used in this part are listed below:

- Government ownership of the project.
- Plant capacity (m) is 8000, 13000, and 17000 $m^3/d$
- Project lifetime (n) is 20 years.
- Interest rate (i) is 5%.
- Electricity cost (c) is $0.05/kWhr.
- Pump efficiency is 85%.
- Recovery ratio is 75%.
- Chemicals cost (k) is $0.033/$m^3$
- Labor cost (l) is $0.05/$m^3$
- Specific power consumption (w) is 2.3, 2.48 and 2.76 kwh/$m^3$
- Plant availability (f) is 0.9.

The cost calculation method that will be followed here was presented by El-Dessouky and Ettouney [2]. Mainly, the method divides the cost into capital (direct and indirect) and operating costs. It describes different cost items under both major categories of the cost, which will be briefly presented here.

**Capital cost**

This comprises all the purchasing costs of land and different types of equipment as well as the buildings and their construction. It also takes into account the cost of membranes and auxiliary equipment. Table 3 details the capital costs considered in the current analysis.

The costs shown in % of the total direct capital cost are known as the indirect capital costs.

**Table 3 Capital cost items.**

| Item | Value |
|---|---|
| Land | 0 |
| Well supply | \$650/m |
| Process equipment | \$500/$m^3$ |
| Buildings | \$500/$m^2$ |
| Freight and Insurance | 5% of DCC |
| Construction overhead | 15% of DCC |
| Owner's costs | 10% of DCC |
| Contingency | 10% of DCC |

**Operating cost:**

These include costs associated with the commissioning of the project and the actual operation period. Table 4 lists the operating costs considered here.

**Table 4 Operating costs items.**

| Item | Value |
|---|---|
| Electricity | \$0.09/kWhr |
| Labor | \$0.05/$m^3$ |
| Membrane replacement | %10/yr of MC |
| Spares & Maintenance | 2% of TCC |
| Insurance | 0.5% of TCC |
| Amortization | Equations |
| Chemicals | \$0.033/$m^3$ |

Amortization and fixed costs are obtained by the following equations:

Amortization factor:

$$a = \frac{i(1\ + i)^n}{(1\ + i)^n - 1}$$

Annual fixed charges:

$$A_1 = a * DCC$$

Annual electricity cost:

$$A_2 = c * w * f * m * 365$$

Annual chemicals cost:

$$A_3 = k * \ f * \ m * 365$$

The total annual cost:

$$A_t = A_1 + A_2 + A_3 + A_4$$

Where, $A_4$ is the annual membrane replacement cost.

The unit production cost will then be obtained from:

$$A_s = \frac{A_t}{f * m * 365}$$

This analysis was then applied under the aforementioned assumptions and input parameters for the system to calculate the cost of water production and the results are presented in section 4.3.

## 3.4 Optimization of the hybrid membrane system

The objective of this part of the work is to optimize the BWRO system for lowest specific energy consumption. The focus in the optimization will be on the recovery ratio and the mixed permeate stream concentration. The optimization will be performed using the engineering equation solver (EES). As this is a single degree of freedom optimization, the recursive quadratic approximation method and the golden section search can be used in EES.

The first is known to be faster while the latter is considered to be more reliable and hence is chosen to be used in the current work. Figure 22 shows the golden section search method.

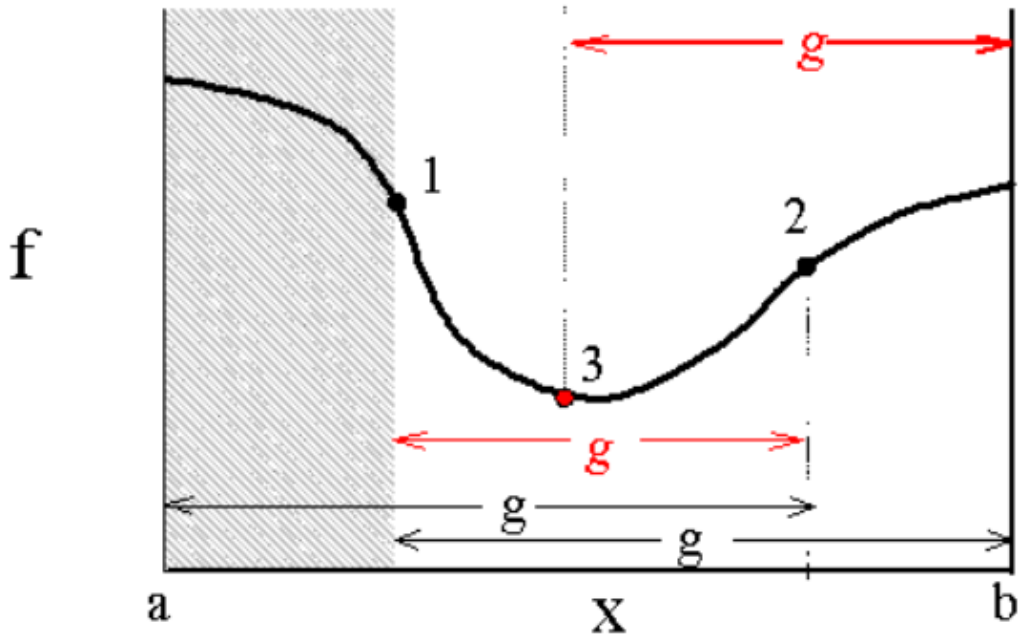


**Figure 22 The golden section search method**

In the figure, a range is specified for the independent variable X. The points a and b represent the initial range. As the iterations take place, a fraction of the range (1-g) of the range is eliminated (the hashed area). Then for the reduced range, the same process is

repeated. The new range points will be from g to the end of the range. Then equations will be solved for g, which is called the golden section which will determine the position of point 3 and then the process is repeated until the search criteria are met.

For this study, the focus will be on the mixed stream of the two water products from the hybrid system. The input parameters are as listed in Table 5. The mixed product concentration was also set and used as an input at the different draw solution concentrations used here.

**Table 5 Optimization study inputs**

| Parameter | Value |
|---|---|
| Feed salinity | 2400 (ppm) |
| Membrane area | 40 ($m^2$) |
| Water permeability coefficient | 1.056 ($L/m^2$ h bar) |
| Pump efficiency | 80 (%) |
| Membrane rejection rate | 99.8 (%) |
| NF RR | 50 (%) |

# CHAPTER 4

# Results and Discussion

## 4.1 Modeling and validation of the system

The graphs below show the validation of the EES simulation results against the results reported by Altaee and Hilal [68]. The variables considered for the validation are the recovery ratio (RR), specific energy consumption ($E_s$), feed pressure ($P_f$), and product concentration ($C_{prod}$) for the NF process, the draw solution concentration (DSC), specific energy consumption, and product quantity ($Q_{prod}$) for the FO process and the feed pressure, draw solution concentration, and specific energy consumption for the RO process. For the overall system performance validation, the total specific power consumption ($Es_t$) and the overall recovery ratio ($RR_t$) are considered and the results are presented.

The validation shows good agreement between the model results and the reference work. The difference between results of the EES and those of the reference work can be attributed to the difference in the properties of the water used in the current model and the reference work.

The following sections will detail the validation results for the three components of the hybrid membrane system.

### 4.1.1 NF process validation

The following three parameters are used in the validation process of the NF system; the feed pressure ($P_f$), the concentration of the product water ($C_{prod}$), and the specific energy consumption ($E_s$). Figure 23 shows the variation of the feed pressure with respect to the recovery ratio RR. Increasing the recovery ratio increased the feed pressure due to the concentration polarization phenomenon.

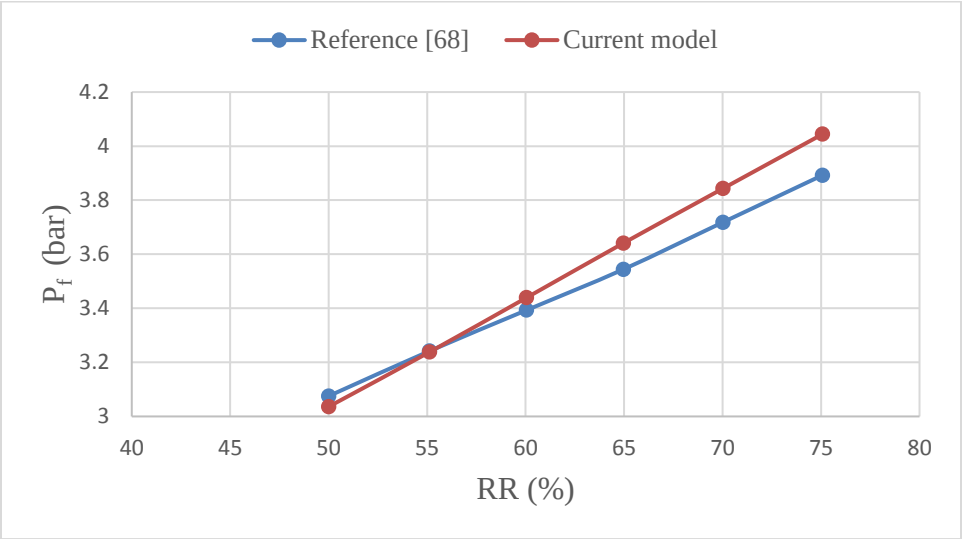


**Figure 23 Feed pressure at different recovery ratios**

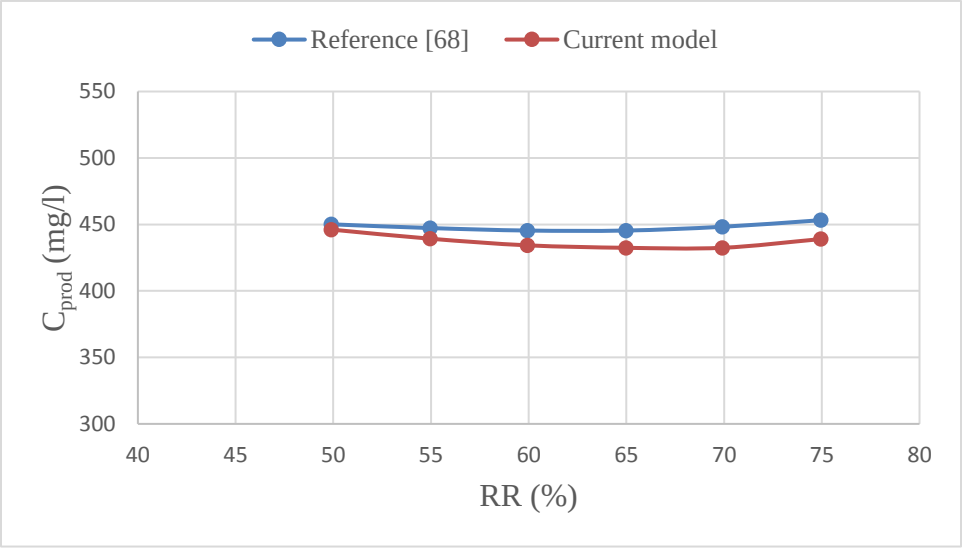


**Figure 24 Permeate concentration at different recovery rates**

As shown in Figure 24 the concentration of the product water changes slightly with the variation in the recovery ratio, increasing at low and high recovery ratios and decreasing in the middle.

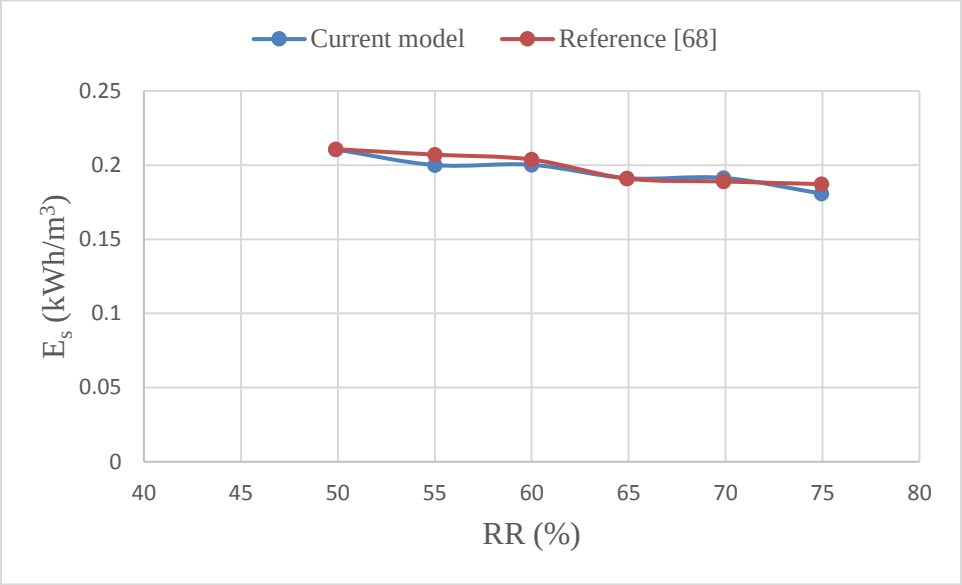


**Figure 25 Specific power consumption at different recovery rates**

The variation of the specific energy consumption with the recovery ratio is presented in Figure 25. It decreases with increasing the recovery ratio as per Equation 4.

### 4.1.2 FO process validation

The following two parameters are used in the validation process of the FO system; the specific energy consumption ($E_s$) and the quantity of the product water ($Q_{prod}$). Figure 26 shows that the specific energy consumption decreases with increasing concentration of the draw solution because of the larger quantity of water that is extracted from the feed stream as shown in Figure 27 due to the higher driving force at higher osmotic pressure differences.

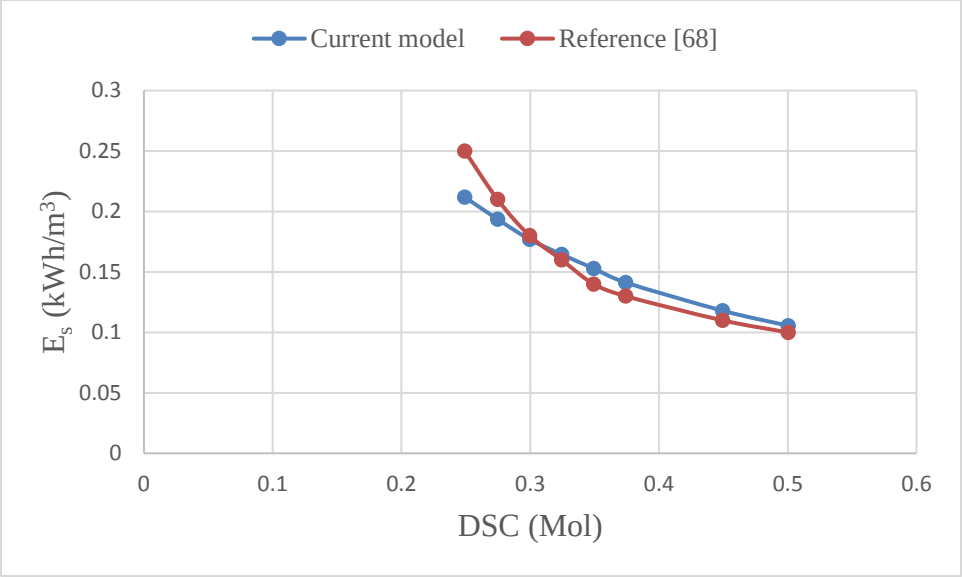


**Figure 26 Specific power consumption at different draw solution concentrations**

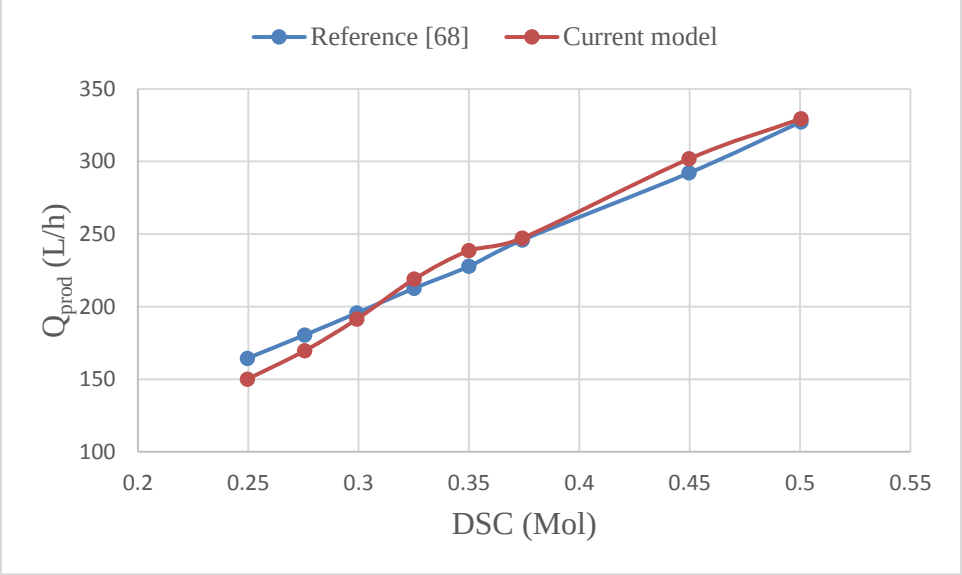


**Figure 27 Permeate flow at different draw solution concentrations**

### 4.1.3 Validation of the RO process

The validation process of the RO system will also use the same three parameters used in the NF validation previously. The concentration of the product water, as shown in Figure 28, increases with the draw solution concentration due to the higher salt diffusion through the membrane as the feed concentration increases.

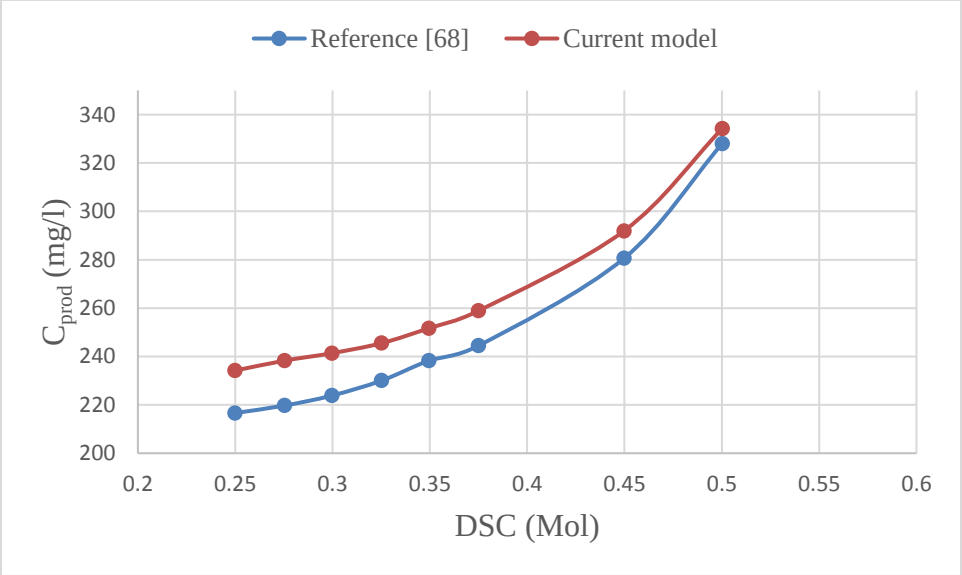


**Figure 28 Permeate concentration at different draw solution concentrations**

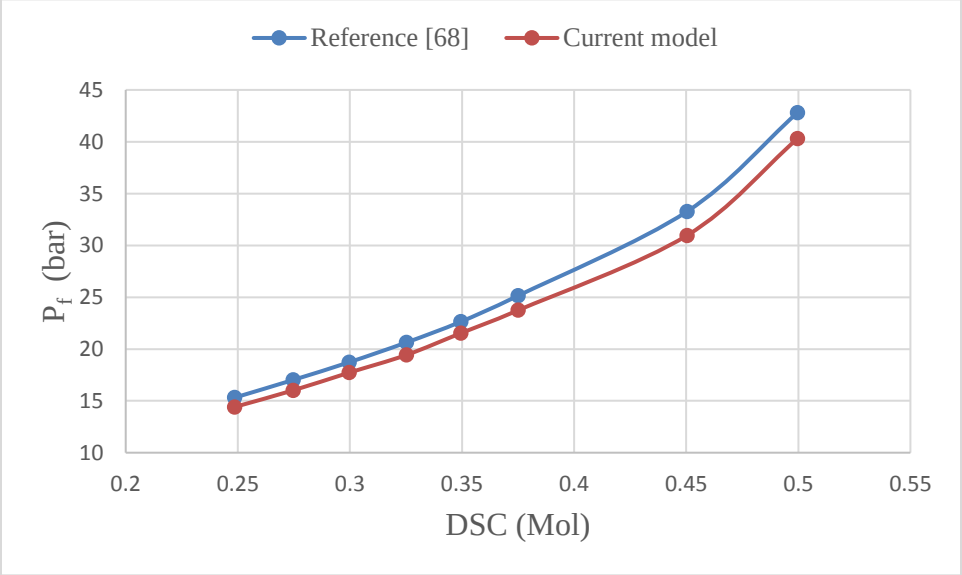


**Figure 29 Feed pressure at different draw solution concentrations**

As shown inn Figure 29, the feed pressure also increases with the concentration of the draw solution because the osmotic pressure to work against increases with increasing feed concentration. As a result of the increase in the feed pressure with the draw solution concentration, the specific energy consumption will follow a similar trend as shown in Figure 30.

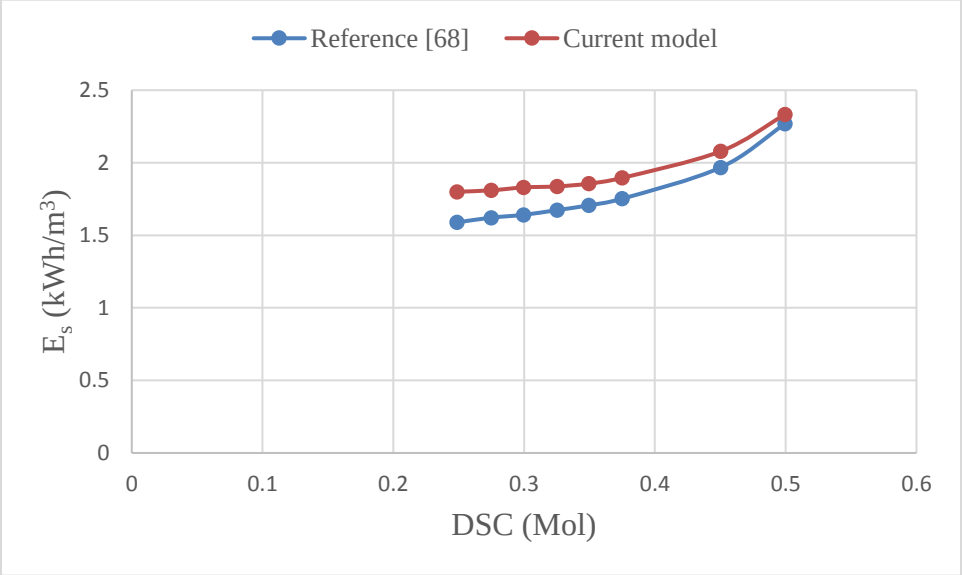


**Figure 30 Specific power consumption at different draw solution concentrations**

### 4.1.4 Validation of the overall NF/FO/RO process

The total specific energy consumption of the overall NF/FO/RO process, which is the sum of specific energy consumption of all three systems, is shown in Figure 31. Specific energy consumption increases with increasing draw solution concentration as the specific energy consumption of both the FO and RO systems increase as it is increased.

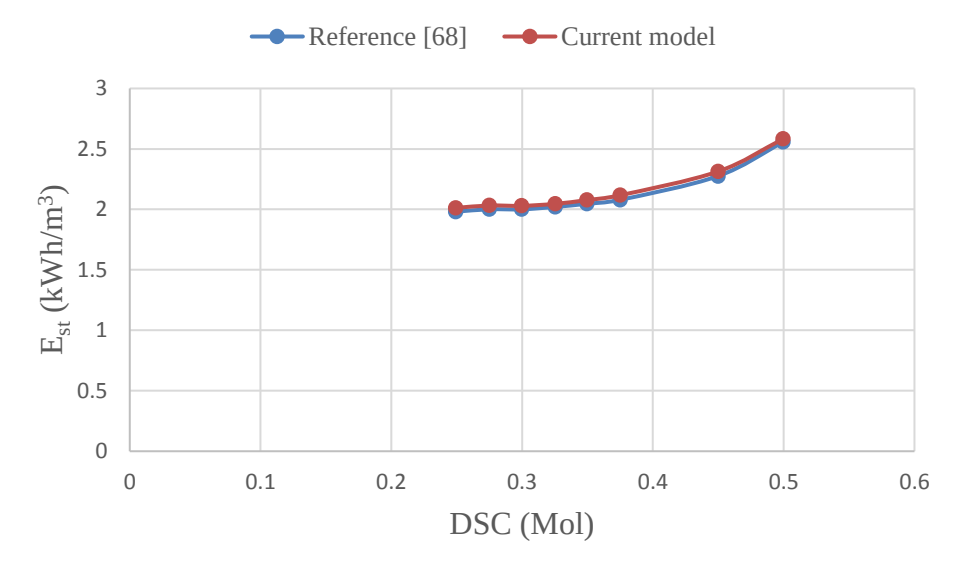


**Figure 31 Specific power consumption at different draw solution concentrations**

## 4.2 Integration with renewable energy sources

The proposed system in this renewable energy coupling feasibility study includes a diesel generator, wind turbines, PV modules, power converter, and a storage system (batteries). This system, based on the data obtained from the EES model, will power the pumps used to operate the membrane system. Figure 32 shows a schematic diagram of the overall integrated system.

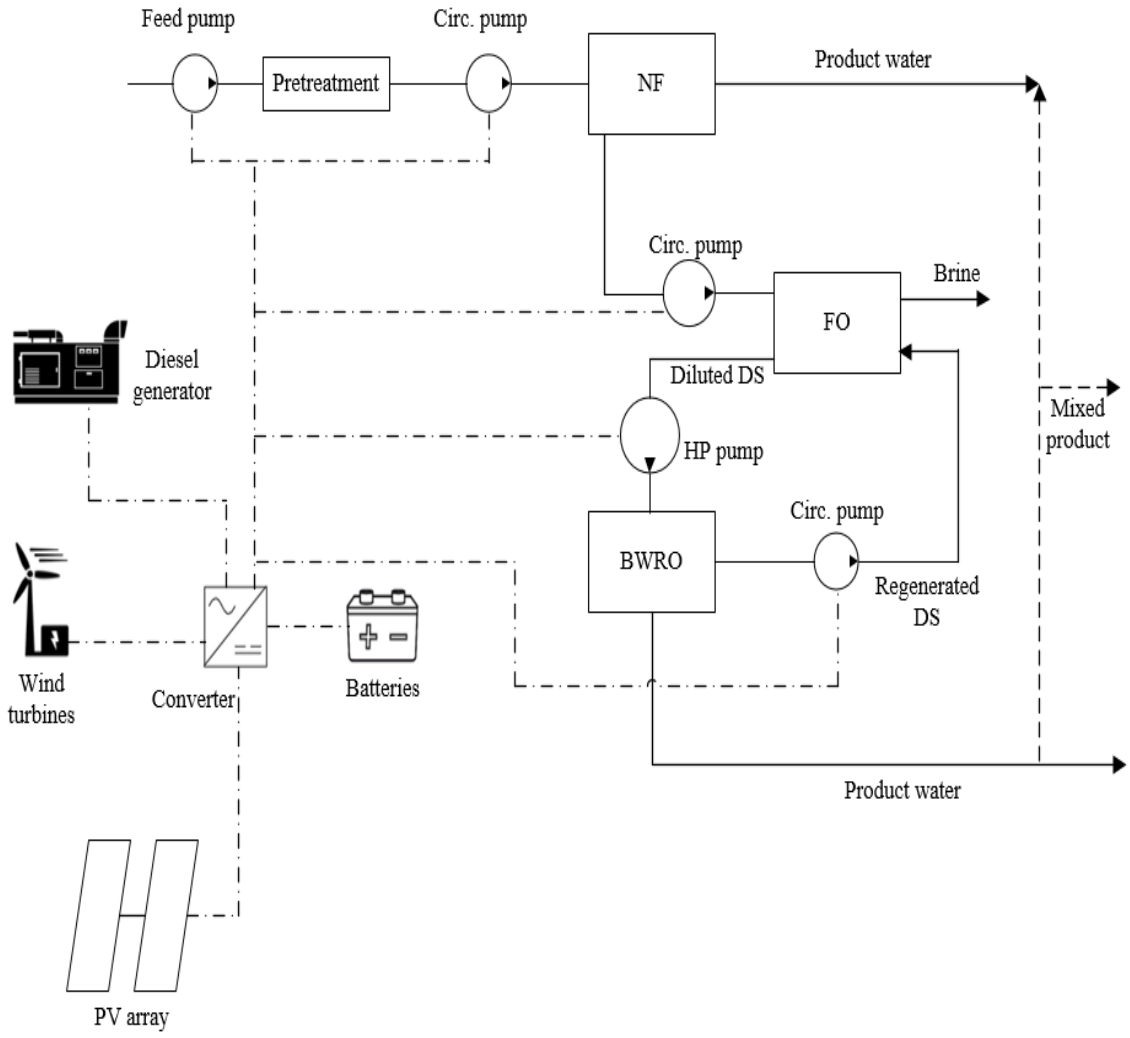


**Figure 32 Integrated system**

Three different locations were considered for this part of the work, each of which has a different system capacity. These locations were selected to cover different climatic regions in Saudi Arabia. Table 6 below details the three locations and their specifications.

**Table 6 Chosen Details of the chosen locations.**

| Location | Water salinity (mg/l) | System capacity ($m^3/d$) | SEC of the membrane system ($kWh/m^3$) |
|---|---|---|---|
| Wadi Dawasir | 3000 | 8000 | 2.3 |
| Qassim | 6000 | 13000 | 2.48 |
| Tabuk | 10000 | 17000 | 2.76 |

The HOMER hybrid system considered for the feasibility study uses the energy load of each one of the three systems, which were obtained at a draw solution concentration of 0.35 Mol and a recovery ratio of 75% from the EES model. The 75% recovery ratio was chosen because it is suitable for this system due to the fact that most brackish water RO desalination systems operate between 70% and 75% recovery ratios [69]. The specific energy consumption obtained from EES was converted to power and used as the input in HOMER for each of the locations. The meteorological data for all three locations were obtained from the website of the national aeronautics and space administration (NASA). The following sections provide the results for each of the three locations.

### 4.2.1 Wadi Dawasir system:

The layout of the system is shown in Figure 33. It shows the main components of the proposed system; a diesel generator, a Vestas V82 wind turbines, PV array, Surrette S4KS25P batteries, and a converter as sketched in HOMER. The wind and solar radiation data for the system in Wadi Dawasir as used in HOMER are shown in Figures 34 and 35, respectively.

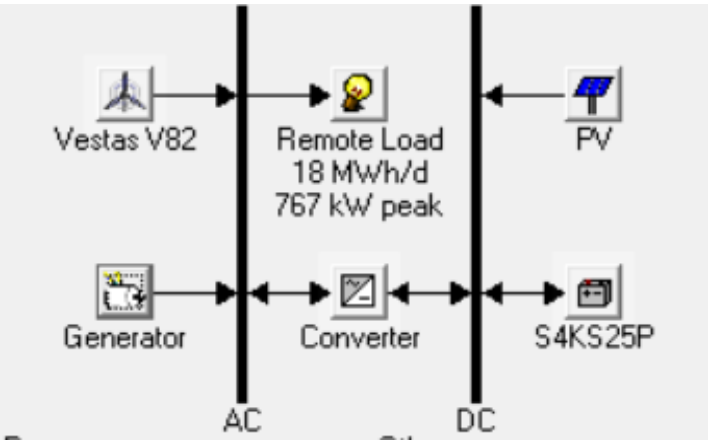


**Figure 33 Overall integration system layout for Wadi Dawasir**

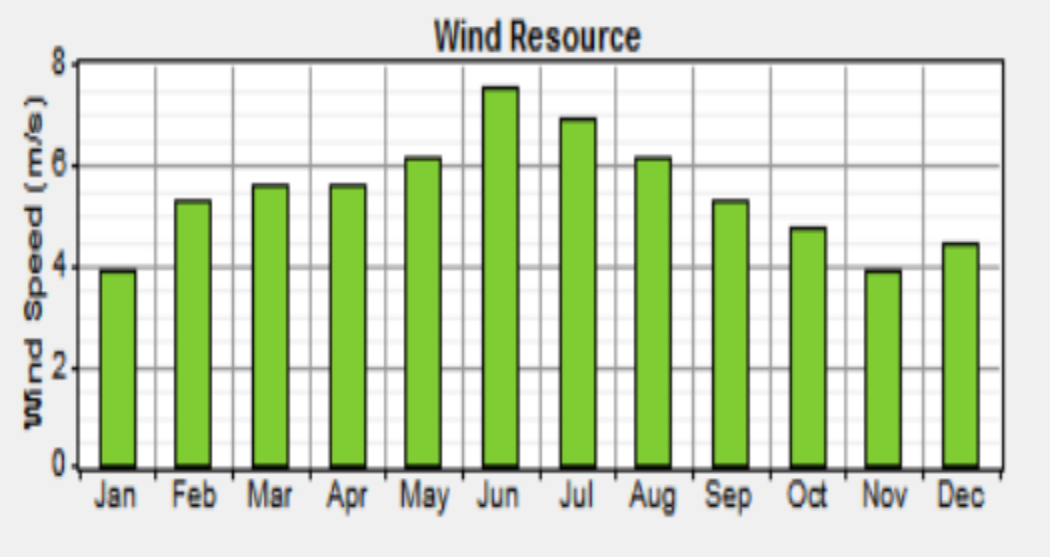


**Figure 34 Wind data for Wadi Dawasir**

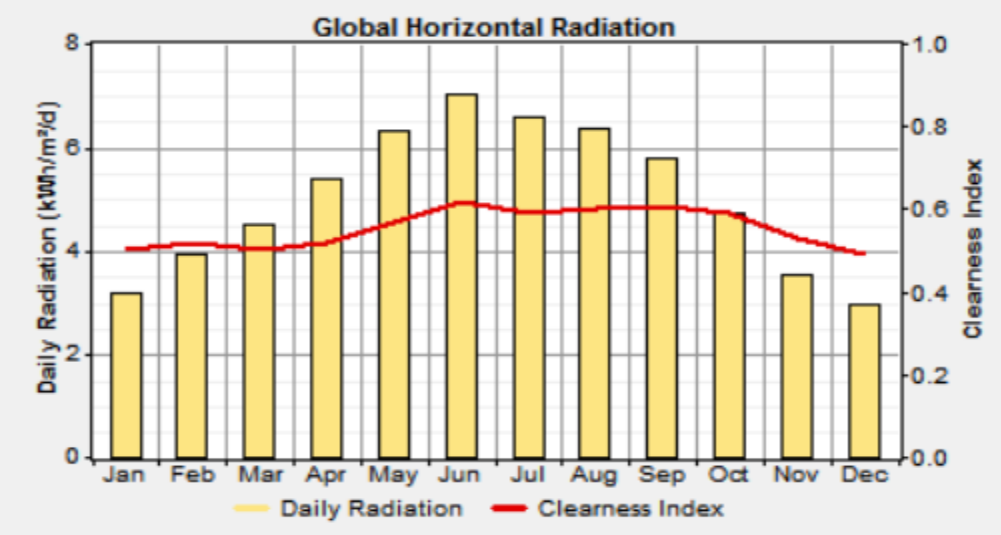


**Figure 35 Solar energy data for Wadi Dawasir**

HOMER also needs detailed information about the specifications of the components of the renewable energy system. The details for Wadi Dawasir system are given below.

Diesel generators

Generator sizes considered: 0 and 1200 kW

Generators lifetime: 20000 hours

Minimum load ratio: 30%

Capital cost of generators: 1000 $/kW

Generators replacement cost: 1000 $/kW

O&M cost: 0.012 $/h

Diesel price: 0.13 $/L

Wind Turbines

Turbines capacity: 1650 kW

Number of turbines considered: 0, 1, 3

Wind turbines lifetime: 20 years

Wind turbine cost: 2000000 $/turbine

Wind turbine replacement cost: 1250000 $/turbine

O&M cost: 20000 $/turbine/year

Power converters (inverter and rectifier)

Sizes considered for the converter: 0 and 500 kW

Converter life time: 15 years

Converter efficiency: 90%

Converter cost: 250 $/kW

Replacement cost: 200 $/kW

O&M cost: 0 $/kW/year

PV modules (panels)

Considered PV sizes: 0, 500, 1000 kW

PV modules lifetime: 20 years

PV modules cost: 1000 $/kW

PV modules replacement cost: 1000 $/kW

O&M cost: 0 $/kW/year

The power load, meteorological data and the specifications of the components listed above were all used as inputs while constructing the system in HOMER. Then simulations were run for all possible combinations seeking all the possible feasible combinations, and listing them and sorting them based on their total net present cost (NPC).

The optimization results obtained with HOMER shown here are for a diesel price of 0.25 $/L and a wind speed of 6 m/s.

For this system capacity and location, the most feasible renewable energy option was to couple the membrane system with diesel/wind configuration and use batteries for a cost of energy (COE) of 0.086 $/kWh and a fraction of renewable energy used of 0.57. The most feasible combination that includes all wind, PV, and diesel components resulted in a COE of 0.095 $/kWh and used a renewable energy fraction of 0.63. The system architectures for both options are given below.

The diesel/wind configuration provides a total net present cost and an annual operation cost of 7.42 M$ and 384946 $/yr, respectively, while the Diesel/Wind/PV configuration provides a total net present cost and an annual operation cost of 8.18 M$ and 365719 $/yr, respectively. The cash flow summary for both systems in Wadi Dawasir are presented in Figure 36. It shows how much each system component contributes to the different costs. In both configurations, the wind turbine was the biggest contributor to capital, operating, and replacement costs, while the diesel cost is the highest of all the costs.

**Table 7 Architecture of the two systems at Wadi Dawasir**

| Option | PV Array | Wind | Generator | Battery | Inverter | Rectifier | Dispatch strategy |
|---|---|---|---|---|---|---|---|
| Diesel/Wind | - | 1 Vestas V82 | 800 kW | 260 Surrette 4KS25P | 500 kW | 500 kW | Cycle Charging |
| Diesel/Wind/PV | 500 kW | 1 Vestas V82 | 800 kW | 260 Surrette 4KS25P | 500 kW | 500 kW | Cycle Charging |

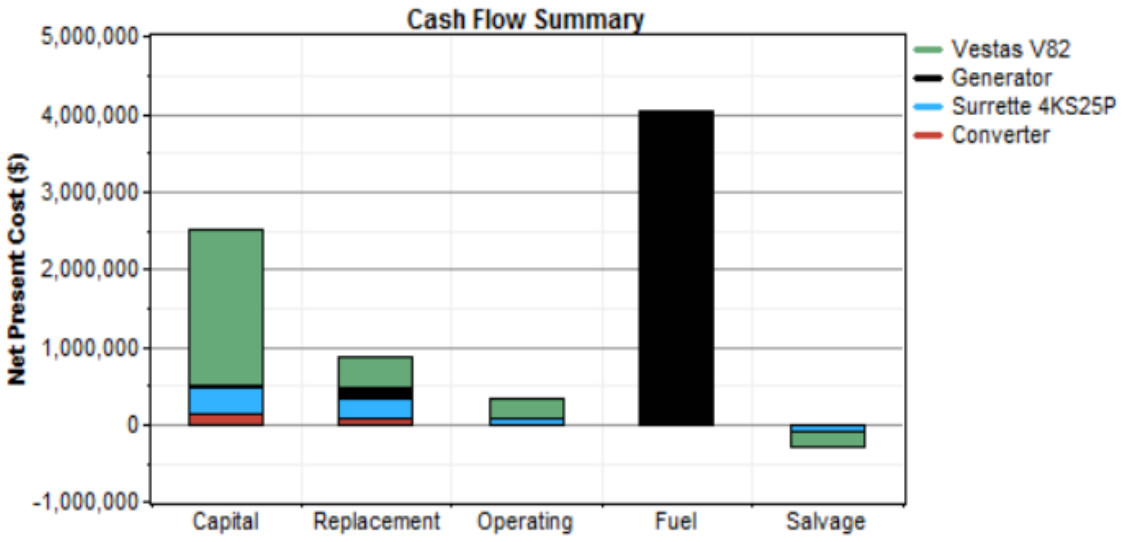


a

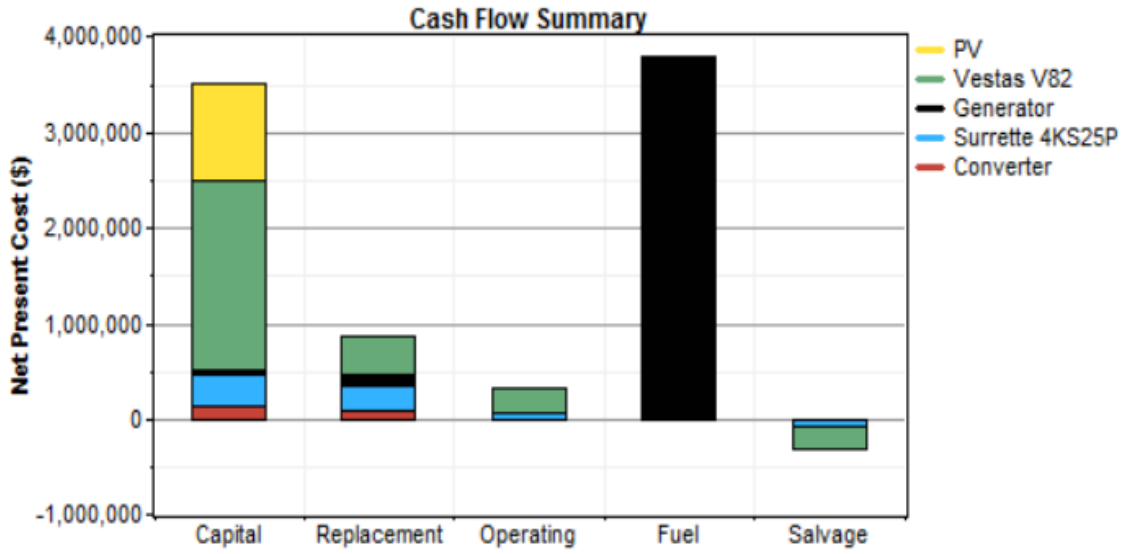


b

**Figure 36 Cash flow summary for a: Diesel/Wind and b: Diesel/Wind/PV in Wadi Dawasir.**

Figure 37 on the other hand represents the monthly average electricity production from the corresponding renewable energy sources. The electricity produced by the wind turbine and the diesel generator decreases with the addition of PV modules in the Diesel/Wind/PV

configuration compared to the Diesel/Wind configuration. The PV contribution to the electricity produced monthly is small compared to that produced by the wind turbine and diesel generator in the Diesel/Wind/PV configuration.

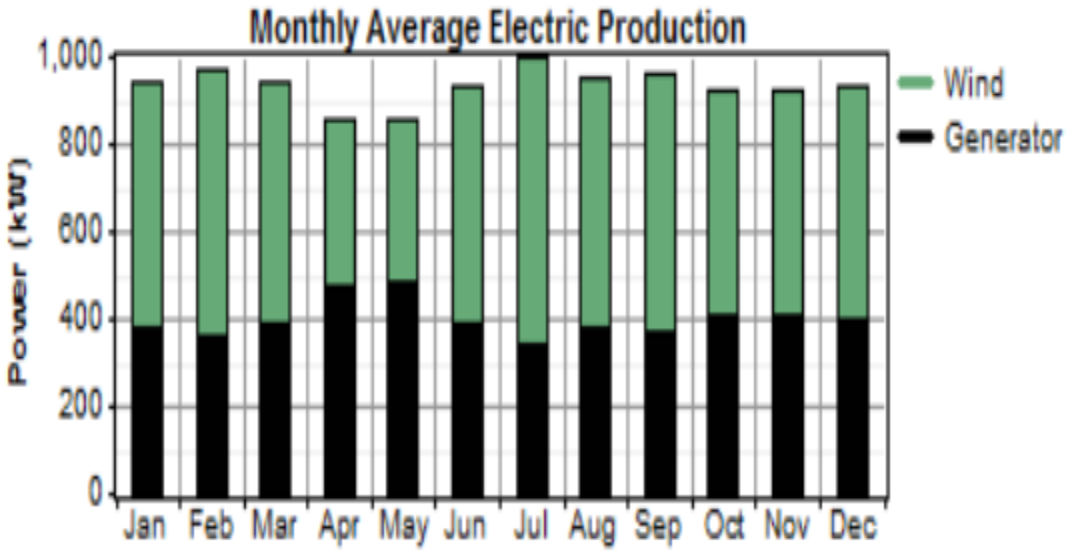


a

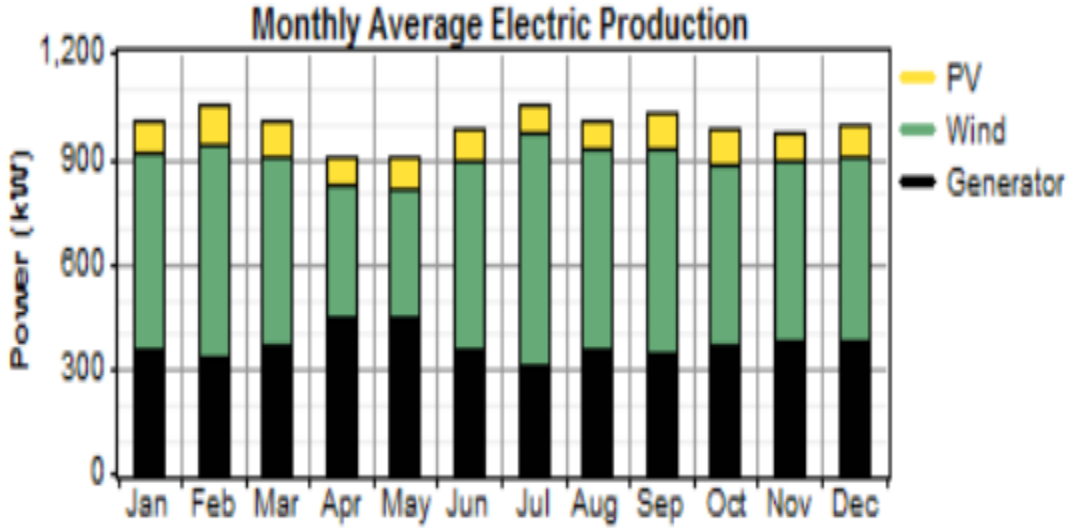


b

**Figure 37 Monthly average electric production for a: Diesel/Wind and b: Diesel/Wind/PV in Wadi Dawasir.**

Tables 8 and 9 below show the production and fractional contribution of each of the system's renewable energy sources while Table 10 lists the amounts of each of six pollutants resulting from the renewable energy coupled system and compares them to the case in which a diesel generator is the sole source of power.

As shown in Tables 8 and 9, wind turbine produces most of the total electricity (57%), while the diesel generator comes second (43%). The electricity produced by both wind turbine and diesel generator decreases when PV modules are added in the Diesel/Wind/PV configuration to produce 10% of the total electricity.

**Table 8 Renewable energy production and fractions for Diesel/Wind configuration in Wadi Dawasir**

| Component | Production | Fraction |
|---|---|---|
| | (kWhr/yr) | % |
| Wind turbine | 4,653,354 | 57 |
| Diesel generator | 3,511,927 | 43 |
| Total | 8,165,281 | 100 |

**Table 9 Renewable energy production and fractions for Diesel/Wind/PV configuration in Wadi Dawasir**

| Component | Production | Fraction |
|---|---|---|
| | (kWhr/yr) | % |
| PV array | 800,535 | 10 |
| Wind turbine | 4,653,354 | 54 |
| Diesel generator | 3,220,962 | 37 |
| Total | 8,674,851 | 100 |

As shown in Table 10, $CO_2$ is the main pollutant produced by the system with other ones being of lesser magnitude for all three configurations. Between the diesel only and Diesel/Wind/PV configurations there is about 50% drop in $CO_2$ emissions.

**Table 10 GHG Emissions for Wadi Dawasir systems**

| Emissions (Ton/yr) | Diesel Generator | Diesel/Wind | DG/PV/Wind |
|---|---|---|---|
| Carbon dioxide | 6,084.1 | 3,331.6 | 3,130.3 |
| Carbon monoxide | 15 | 8.2 | 7.7 |
| Unburned hydrocarbons | 1.7 | 0.9 | 0.85 |
| Particulate matter | 1.1 | 0.6 | 0.58 |
| Sulfur dioxide | 12.2 | 6.7 | 6.3 |
| Nitrogen oxides | 134 | 73.3 | 68.9 |

### 4.2.2 Qassim system:

The layout of the system is shown in Figure 38. It shows the main components of the proposed system; a diesel generator, a Vestas V82 wind turbines, PV array, Surrette S4KS25P batteries, and a converter as sketched in HOMER. The wind and solar radiation data for the system in Qassim as used in HOMER are shown in Figures 39 and 40, respectively.

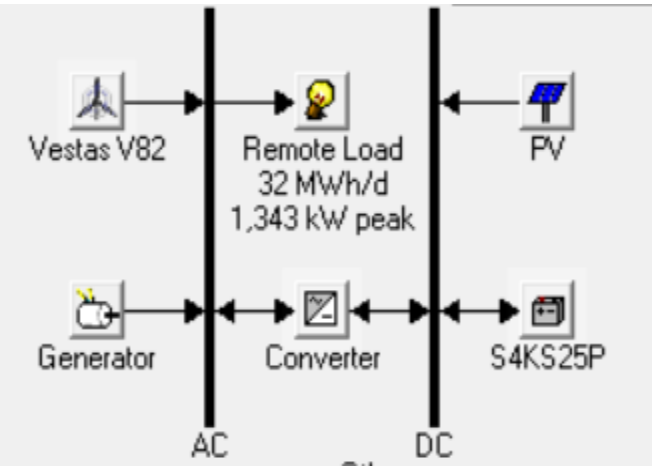


**Figure 38 Overall integration system layout for Qassim**

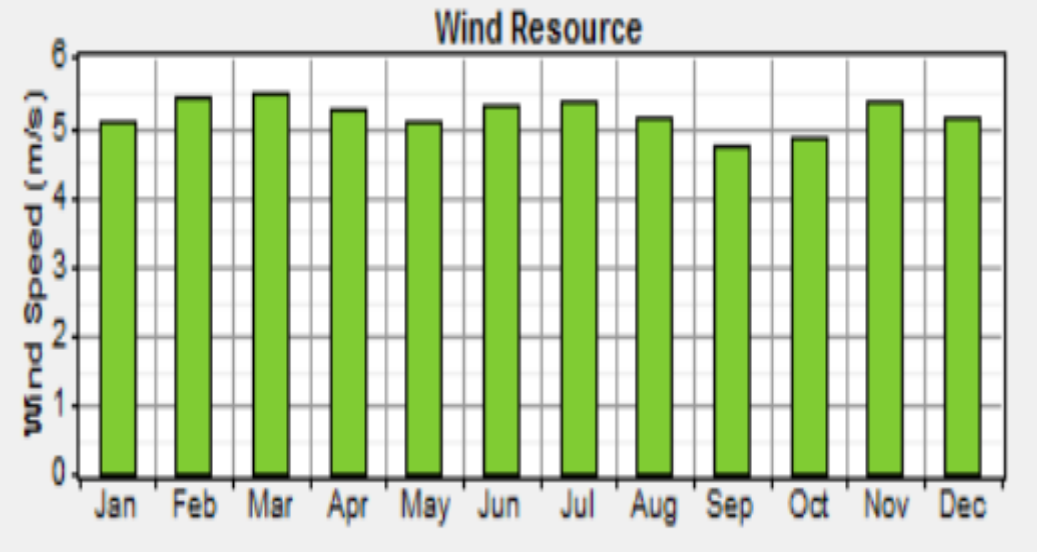


**Figure 39 Wind data for Qassim**

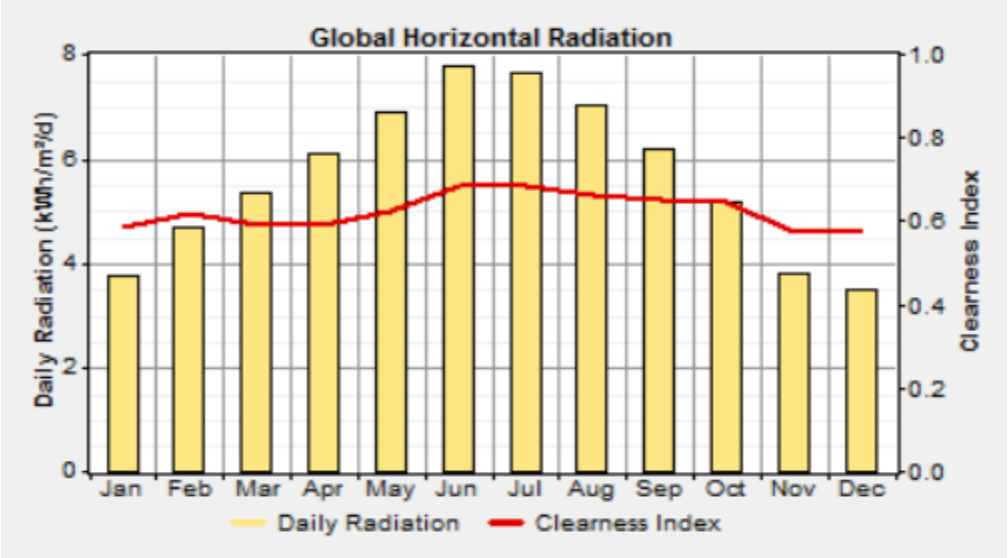


**Figure 40 Solar energy data for Qassim**

HOMER also needs detailed information about the specifications of the components of the renewable energy system. The details for Qassim system are given below.

Diesel generators

Generator sizes considered: 0, 900, 1500, 2000, and 2500 kW

Generators lifetime: 20000 hours

Minimum load ratio: 30%

Capital cost of generators: 1520 $/kW

Generators replacement cost: 1520 $/kW

O&M cost: 0.012 $/h

Diesel price: 0.13 $/L

Wind Turbines

Turbines capacity: 1650 kW

Number of turbines considered: 0, 6, 8

Wind turbines lifetime: 20 years

Wind turbine cost: 2000000 $/turbine

Wind turbine replacement cost: 1250000 $/turbine

O&M cost: 20000 $/turbine/year

Power converters (inverter and rectifier)

Sizes considered for the converter: 0, 500, 1000, 1200, 1300, 1400, 1500, 1600, 1700, 1800 and 2000 kW

Converter life time: 15 years

Converter efficiency: 90%

Converter cost: 250 $/kW

Replacement cost: 200 $/kW

O&M cost: 0 $/kW/year

PV modules (panels)

Considered PV sizes: 0, 500, 2200, 2300, 2400, 2500, 3000, 3500, 3750, 4000, 4250, 4750, 5000, 5500, 5750, 6000, 6250, 6750, and 7000 kW

PV modules lifetime: 20 years

PV modules cost: 1000 $/kW

PV modules replacement cost: 1000 $/kW

O&M cost: 0 $/kW/year

The power load, meteorological data, and the specifications of the components listed above were all used as inputs to construct the system in HOMER. Then the simulations were run for all possible combinations seeking all possible feasible combinations, listing them and sorting them based on their total net present cost (NPC).

The optimization results obtained with HOMER shown here are for a diesel price of 0.25 $/L and a wind speed of 6 m/s.

For this system capacity and location, the most feasible renewable energy option is to couple the membrane system with a Diesel/PV configuration for a cost of energy (COE) of 0.089 $/kWh and a fraction of renewable energy used of 0.07. The most feasible simulation that includes all wind, PV, and diesel components resulted in a COE of 0.14 $/kWh and a renewable energy fraction of 0.87. The system architecture for both options are given below.

**Table 11 Architecture of the two systems at Qassim**

| Option | PV Array | Wind | Generator | Battery | Inverter | Rectifier | Dispatch strategy |
|---|---|---|---|---|---|---|---|
| Diesel/PV | 500 kW | - | 1500 kW | - | 500 kW | 500 kW | Cycle Charging |
| Diesel/Wind/PV | 500 kW | 6 Vestas V82 | 1500 kW | 140 Surrette 4KS25P | 500 kW | 500 kW | Cycle Charging |

The Diesel/PV configuration provides a total net present cost and an annual operation cost of 13.31 M$ and 0.99 M$/yr, respectively, while the Diesel/Wind/PV configuration provides a total net present cost and an annual operation cost of 21.03 M$ and 633323 $/yr, respectively.

The cash flow summary for both systems in Qassim are presented in Figure 41. It shows how much each system component contributes to the different costs. In the Diesel/PV configuration, the elimination of the wind turbine resulted in a massive drop in the capital,

operating, and replacement costs compared to the Diesel/Wind/PV configuration. While the diesel cost is the greatest of all the costs in the Diesel/PV configuration, the capital cost is the greatest in the Diesel/Wind/PV configuration.

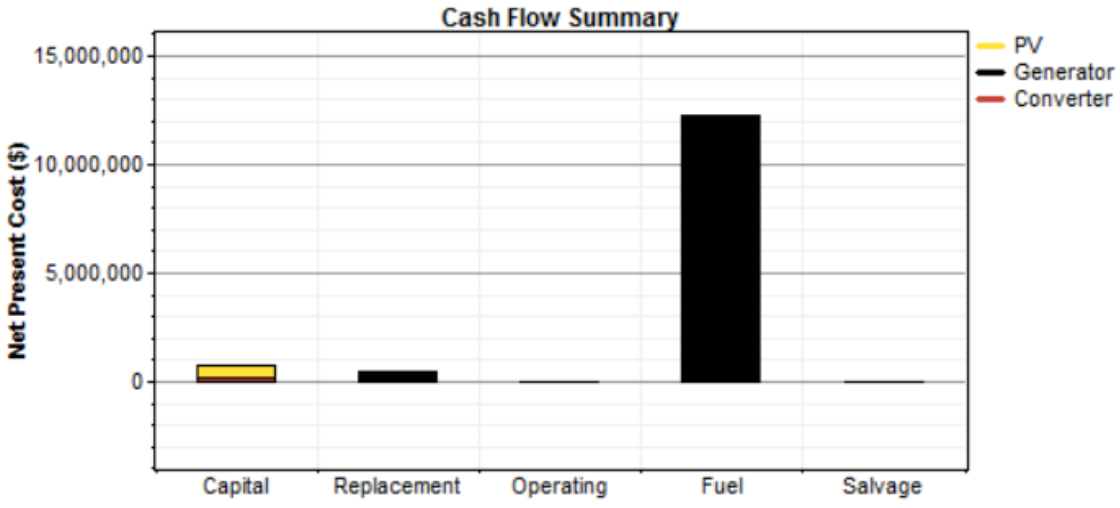


a

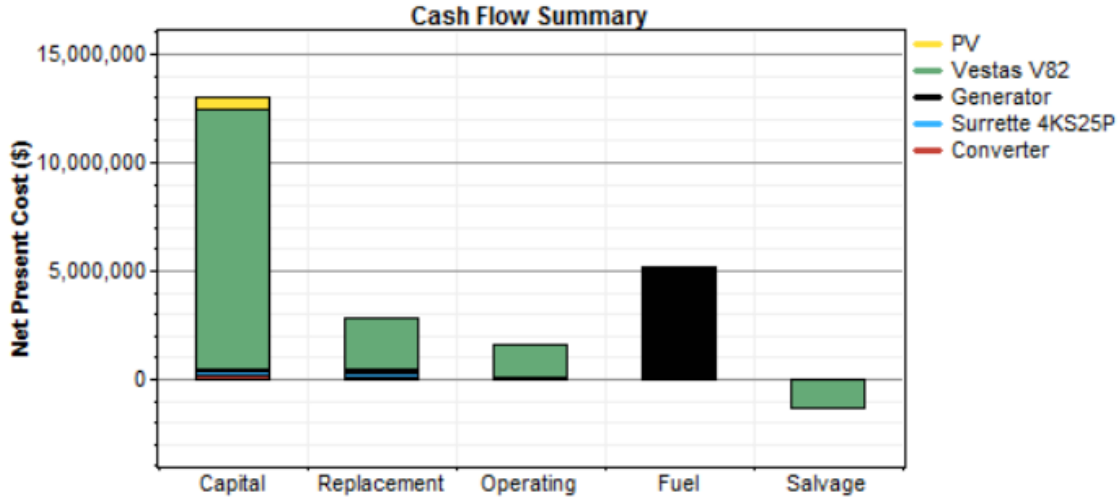


b

**Figure 41 Cash flow summary for a: Diesel/PV and b: Diesel/Wind/PV in Qassim.**

Figure 42 on the other hand provides the monthly average electricity production from the corresponding renewable energy sources. In the Diesel/PV, the electricity produced

monthly by the PV modules is small and even decreased more in the Diesel/Wind/PV configuration. This is because, with the available solar radiation at Qassim producing more electricity from PV modules would be more expensive than from diesel or a wind turbine and hence not feasible.

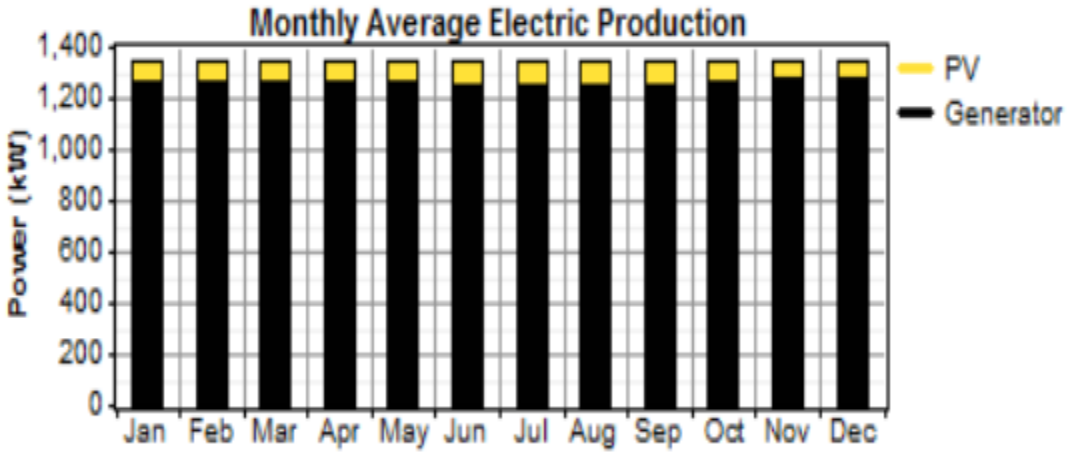


a

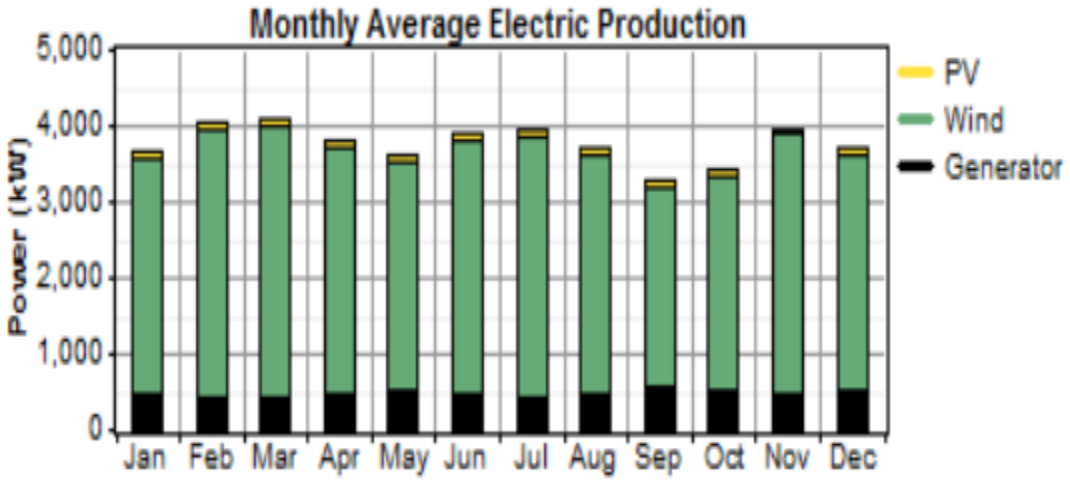


b

**Figure 42 Monthly average electric production for a: Diesel/PV and b: Diesel/Wind/PV in Qassim.**

Tables 12 and 13 show the production and fractional contribution of each of the renewable energy sources, while Table 14 lists the amounts of each of six pollutants resulting from

the renewable energy coupled system and compares them to the case in which a diesel generator is the sole source of power.

As shown in Tables 12, the diesel generator produces most of the total electricity (93%), while as shown in Table 13, wind turbine produces most of the electricity (85%). The electricity produced by both PV and the diesel generator decreases when a wind turbine was added in the Diesel/Wind/PV configuration to produce most of the total produced electricity.

**Table 12 Renewable energy production and fractions for Diesel/Wind configuration in Qassim**

| Component | Production | Fraction |
|---|---|---|
| | (kWhr/yr) | % |
| PV array | 774,859 | 7 |
| Diesel generator | 11,067,343 | 93 |
| Total | 11,842,202 | 100 |

**Table 13 Renewable energy production and fractions for Diesel/Wind/PV configuration in Qassim**

| Component | Production | Fraction |
|---|---|---|
| | (kWhr/yr) | % |
| PV array | 774,859 | 2 |
| Wind turbine | 27,976,112 | 85 |
| Diesel generator | 4,967,112 | 13 |
| Total | 32,983,848 | 100 |

As shown in Table 14, $CO_2$ is the main pollutant produced by the system for all three configurations, with other ones being of lesser magnitude. Between the diesel only and Diesel/Wind/PV configurations there is more than 50% drop in $CO_2$ emissions.

**Table 14 GHG Emissions for Qassim systems**

| Emissions (ton/yr) | Diesel Generator | Diesel/PV | DG/PV/Wind |
|---|---|---|---|
| Carbon dioxide | 10,513.2 | 10,054.1 | 4,219.9 |
| Carbon monoxide | 26 | 24.8 | 10.4 |
| Unburned hydrocarbons | 2.9 | 2.7 | 1.1 |
| Particulate matter | 2 | 1.8 | 0.8 |
| Sulfur dioxide | 21.1 | 20.2 | 8.4 |
| Nitrogen oxides | 231.6 | 221.4 | 92.9 |

### 4.2.3 Tabuk system:

The layout of the system is shown in Figure 43. It shows the main components of the proposed system; a diesel generator, a Vestas V82 wind turbines, PV array, Surrette S4KS25P batteries, and a converter as sketched in HOMER. The wind and solar radiation data for the system in Tabuk location as used in HOMER are shown in Figures 44 and 45, respectively.

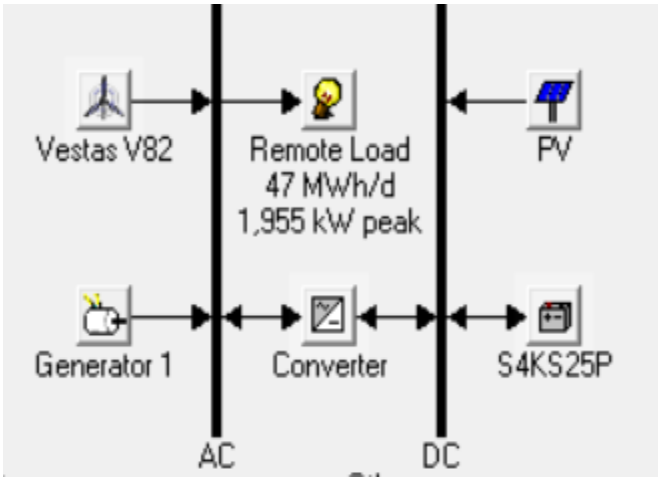


**Figure 43 Overall integration system layout for Tabuk**

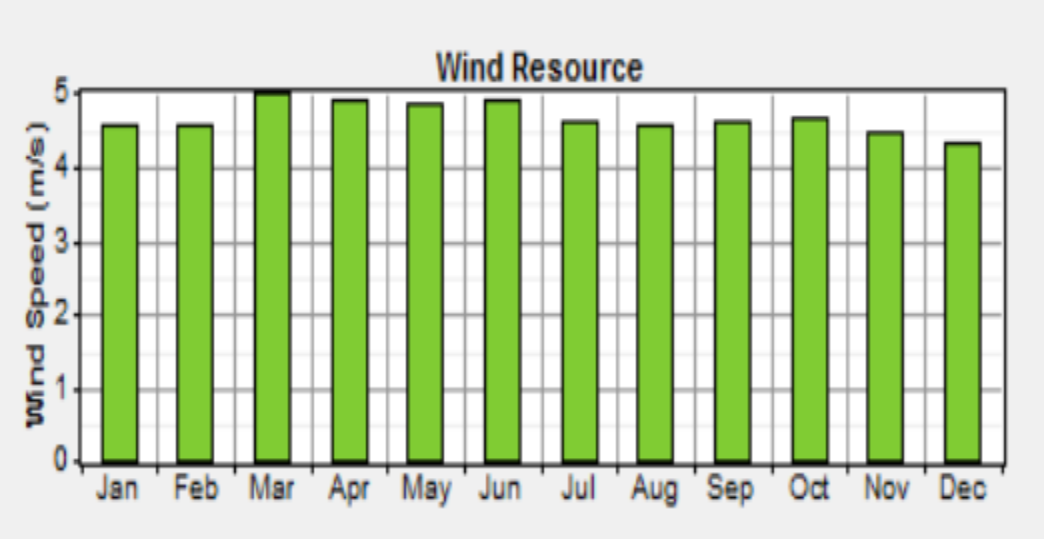


**Figure 44 Wind data for Tabuk**

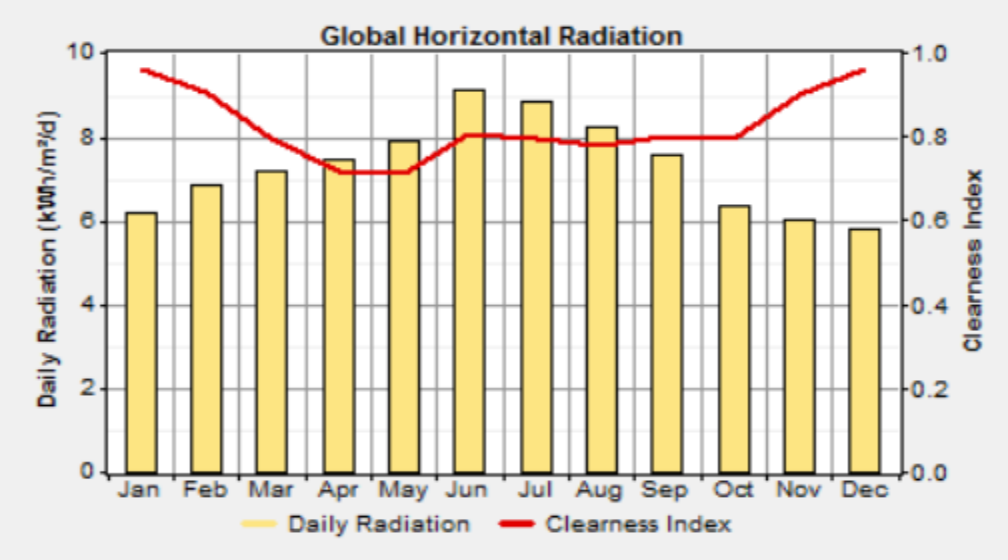


**Figure 45 Solar energy data for Tabuk**

HOMER also needs detailed information about the specifications of the components of the renewable energy system. The details for the Tabuk system are given below.

Diesel generators

Generator sizes considered: 0, 900, 1500, 2000, and 2500 kW

Generators lifetime: 20000 hours

Minimum load ratio: 30%

Capital cost of generators: 1000 $/kW

Generators replacement cost: 1000 $/kW

O&M cost: 0.012 $/h

Diesel price: 0.13 $/L

Wind Turbines

Turbines capacity: 1650 kW

Number of turbines considered: 0, 6, 8

Wind turbines lifetime: 20 years

Wind turbine cost: 2000000 $/turbine

Wind turbine replacement cost: 1250000 $/turbine

O&M cost: 20000 $/turbine/year

Power converters (inverter and rectifier)

Sizes considered for the converter: 0, 500, 1000, 1200, 1300, 1400, 1500, 1600, 1700, 1800, and 2000 kW

Converter life time: 15 years

Converter efficiency: 90%

Converter cost: 250 $/kW

Replacement cost: 200 $/kW

O&M cost: 0 $/kW/year

PV modules (panels)

Considered PV sizes: 0, 500, 2200, 2300, 2400, 2500, 3000, 3500, 3750, 4000, 4250, 4750, 5000, 5500, 5750, 6000, 6250, 6750, and 7000 kW

PV modules lifetime: 20 years

PV modules cost: 1000 $/kW

PV modules replacement cost: 1000 $/kW

O&M cost: 0 $/kW/year

The power load, meteorological data and the specifications of the components listed above were all used as inputs while constructing the system in HOMER. Then simulations were run for all possible combinations seeking all the possible feasible combinations, listing them and sorting them based on their total net present cost (NPC).

The optimization results obtained with HOMER shown here are for a diesel price of 0.25 $/L and a wind speed of 6 m/s.

For this system capacity and location, the most feasible renewable energy option is to couple the membrane system with a Diesel/PV array and use batteries for a cost of energy (COE) of 0.087 $/kWh and a fraction of renewable energy used of 0.05. The most feasible simulation that includes all wind, PV, and diesel components resulted in a COE of 0.112 $/kWh and a fraction of renewable energy used of 0.80. The system architecture for both options are given below.

**Table 15 Architecture of the two systems for Tabuk**

| Option | PV Array | Wind | Generator | Battery | Inverter | Rectifier | Dispatch strategy |
|---|---|---|---|---|---|---|---|
| Diesel/PV | 500 kW | - | 2000 kW | 140 Surrette 4KS25P | 500 kW | 500 kW | Cycle Charging |
| Diesel/Wind/PV | 500 kW | 6 Vestas V82 | 1500 kW | 150 Surrette 4KS25P | 500 kW | 500 kW | Cycle Charging |

The Diesel/PV configuration provides a total net present cost and an annual operation cost of 14.82 M$ and 1.09 M$/yr, respectively, while the Diesel/Wind/PV configuration provides a total net present cost and an annual operation cost of 21.72 M$ and 691,040 $/yr, respectively.

The cash flow summary for both systems in Tabuk are presented in Figure 46. It shows how much each system component contributes to the different costs. In the Diesel/PV

configuration, the elimination of the wind turbine resulted in a massive drop in the capital, operating, and replacement costs compared to the Diesel/Wind/PV configuration. While the diesel cost is the highest of all the costs in the Diesel/PV configuration, the capital cost is the highest in the Diesel/Wind/PV configuration.

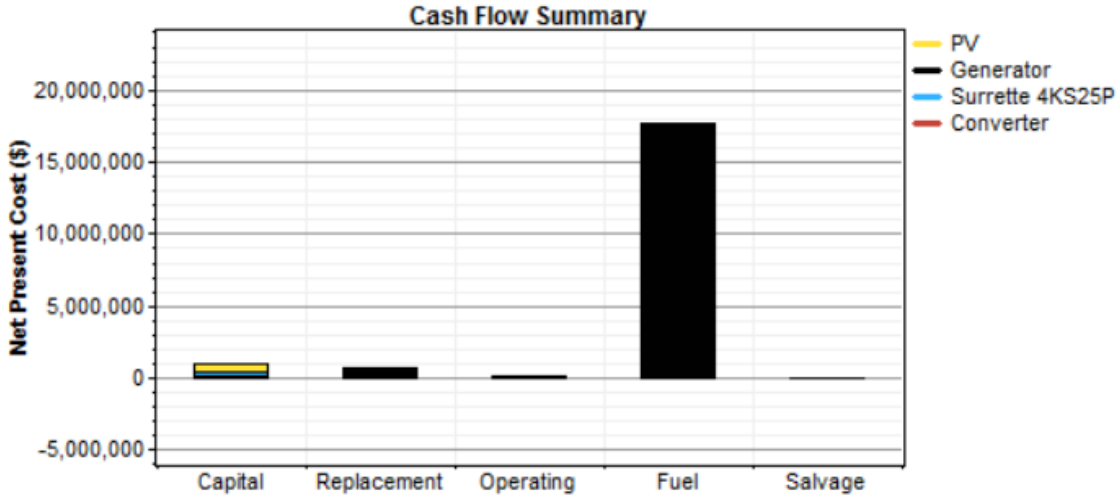


a

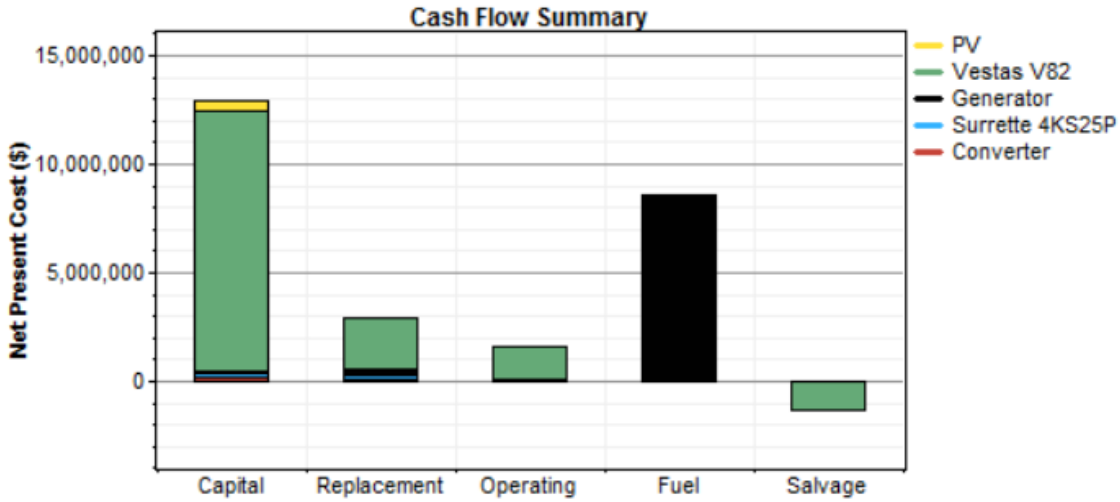


b

**Figure 46 Cash flow summary for a: Diesel/PV and b: Diesel/Wind/PV in Tabuk**

Figure 47 on the other hand represents the monthly average electricity production from the corresponding renewable energy sources. For the Diesel/PV configuration, the electricity produced monthly by the PV modules is small and even decreased more in the Diesel/Wind/PV configuration. This is because, for the available solar radiation in Tabuk, producing more electricity from PV modules would be more expensive than from diesel or a wind turbine and hence not feasible.

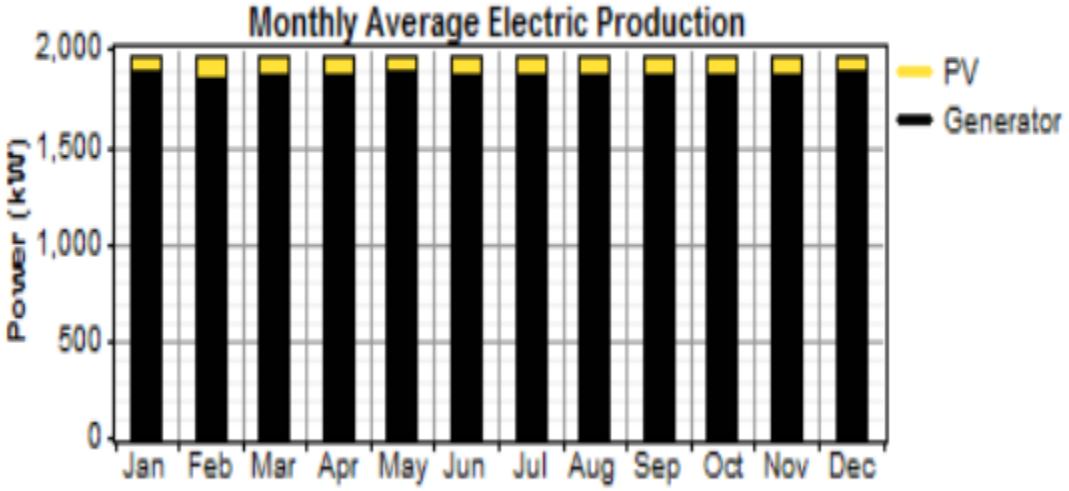


a

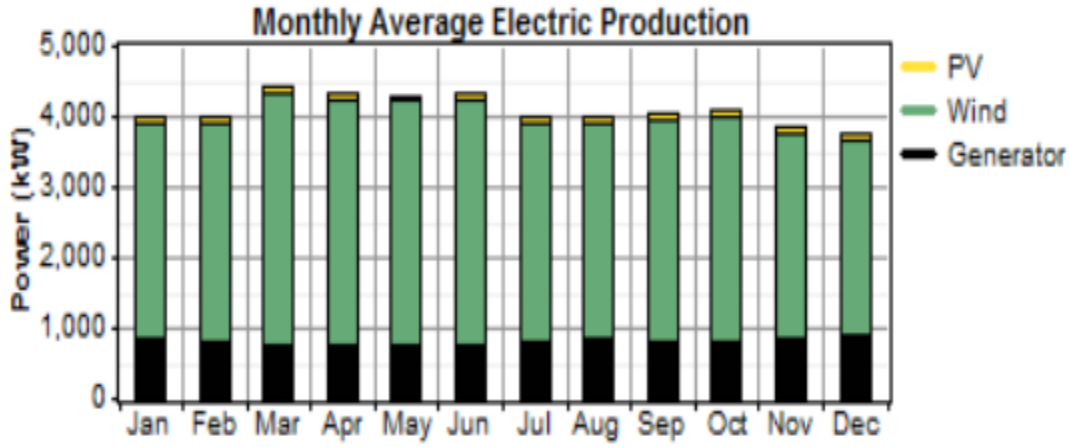


b

**Figure 47 Monthly average electric production for a: Diesel/PV and b: Diesel/Wind/PV in Tabuk.**

Tables 16 and 17 show the production and fractional contribution of each renewable energy source of the system, while Table 18 lists the amounts of each of the six pollutants resulting from the renewable energy coupled system and compares them to the case in which a diesel generator is the sole source of power.

As shown in Table 16 for the Diesel/Wind configuration, diesel generator produces most of the total electricity (95%), while as shown in Table 17 for the Diesel/Wind/PV configuration, the wind turbine produced the most electricity (87%). The electricity produced by both PV and the diesel generator decreased when wind turbine was added in the Diesel/Wind/PV configuration to produce most of the total produced electricity.

**Table 16 Renewable energy production and fractions for Diesel/Wind configuration in Tabuk**

| Component | Production | Fraction |
|---|---|---|
| | (kWhr/yr) | % |
| PV array | 816,623 | 5 |
| Diesel generator | 16,390,742 | 95 |
| Total | 17,207,364 | 100 |

**Table 17 Renewable energy production and fractions for Diesel/Wind/PV configuration in Tabuk**

| Component | Production | Fraction |
|---|---|---|
| | (kWhr/yr) | % |
| PV array | 816,623 | 2 |
| Wind turbine | 27,968,712 | 87 |
| Diesel generator | 7,158,893 | 20 |
| Total | 35,944,228 | 100 |

As shown in Table 18, $CO_2$ is the main pollutant produced by the system in all three configurations, with other pollutants being of lesser magnitude. Between the diesel only and Diesel/Wind/PV configurations there is more than 50% drop in $CO_2$ emissions.

**Table 18 GHG Emissions for Tabuk systems**

| Emissions (ton/yr) | Diesel Generator | Diesel/PV | DG/PV/Wind |
|---|---|---|---|
| Carbon dioxide | 15,886.3 | 14,480.7 | 7,081.2 |
| Carbon monoxide | 39.2 | 35.7 | 17.5 |
| Unburned hydrocarbons | 4.3 | 4 | 1.9 |
| Particulate matter | 3 | 2.7 | 1.3 |
| Sulfur dioxide | 31.9 | 29.1 | 14.2 |
| Nitrogen oxides | 350 | 318.9 | 156 |

## 4.3 Cost analysis

The El-Dessouky method was used to estimate to cost of water production using the hybrid NF/FO/RO system applying the assumptions and cost elements presented in section 3.3. The water production cost for the BWRO systems ranges between 0.14 to 0.38 $/m^3$.

The resulting cost estimates for the hybrid system using the El-Dessouky method were 0.61, 0.56, and 0.55 $/m^3$ for the systems in Wadi Dawasir, Qassim, and Tabuk, respectively. Although the specific energy consumption of the system increased with increasing feed salinity, the product water cost decreased with increasing system capacity.

Figure 48 shows a representation of the cost of product water for the hybrid NF/FO/RO system at each of the three considered locations.

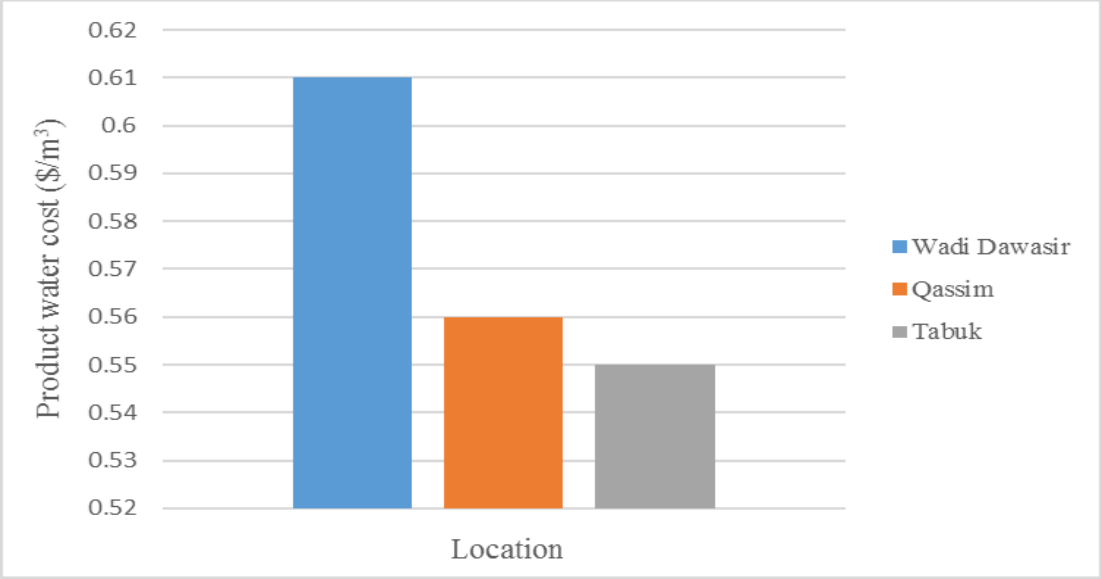


**Figure 48 Water production cost**

## 4.4 Optimization results

The results of the optimization of the hybrid membrane system are shown in Figure 49.

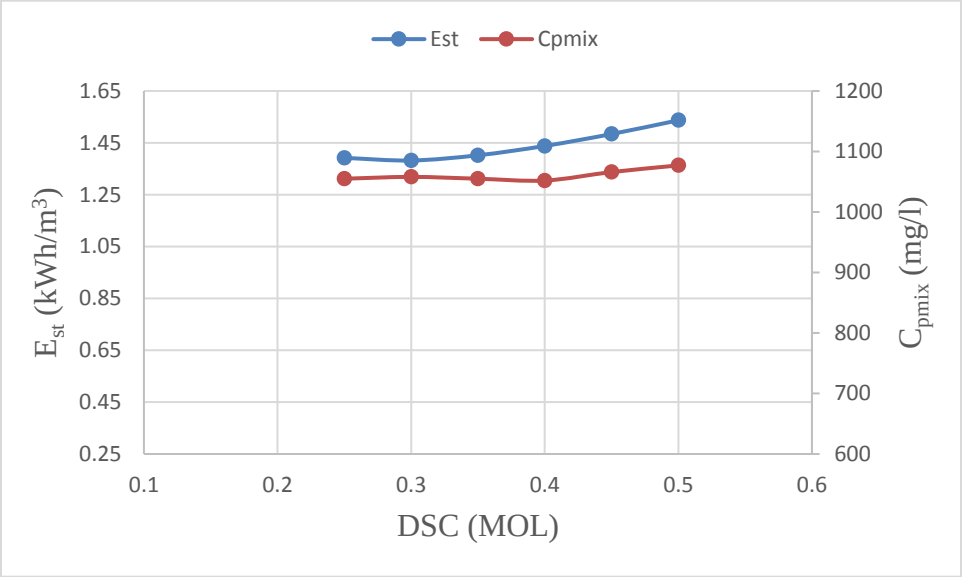


**Figure 49 Hybrid membrane system optimization**

These results show that the optimum operation of the hybrid NF/FO/RO desalination system is governed by the desired product water quality. That is represented here by the salt concentration of the mixed stream of the product waters from the NF and RO systems. It is obvious that the use of a product water with such quality will be limited to non-drinking applications.

For the range of draw solution that was considered here, two options for operation may be of interest; (i) a draw solution concentration 0.25 MOL achieving a specific energy consumption of 1.39 kWh/m$^3$ at 1055 mg/l and (ii) a draw solution concentration 0.3 MOL achieving a specific energy consumption of 1.38 kWh/m$^3$ at 1058 mg/l. The first being the lowest SEC and the second resulting in the lowest permeate concentration.

For the case in which drinking water is also a desired product of the hybrid desalination system and its properties to be optimized, a separate and similar optimization will have to be performed on the NF system first and then the FO/RO system can be also treated separately. In such a case, the product concentration of the two streams will be separately set and then the desired performance parameters will be optimized.

Figure 50 shows this step for the NF system alone.

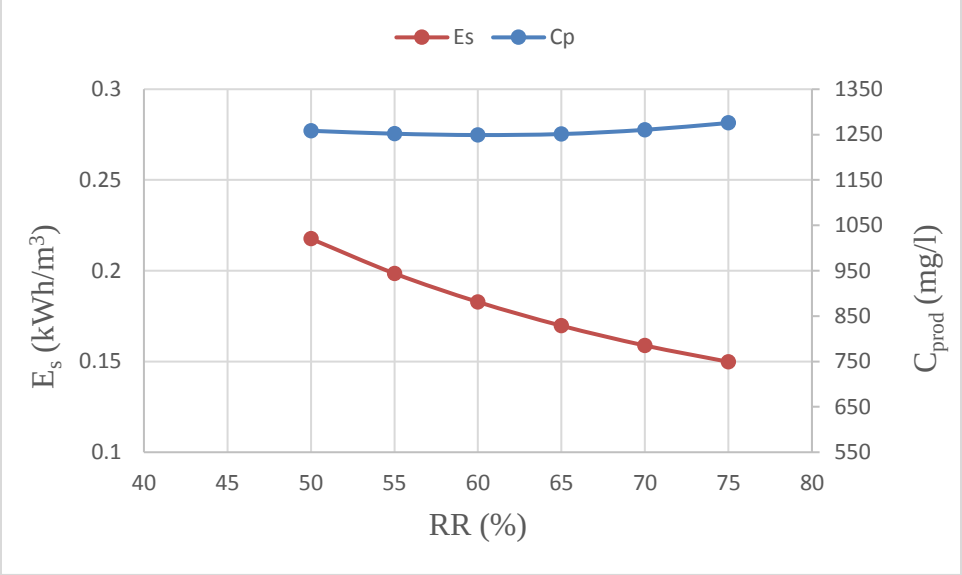


**Figure 50 NF membrane system optimization**

As shown in Figure 50, the variation in the product water concentration is a minimum and hence the optimal operation (lowest specific energy consumption), for the range of recovery ratio that was considered, can be achieved by operating the NF system at the highest recovery ratio possible as long as the permeate concentration is within the allowed range for the specific application.

# CHAPTER 5

# Conclusions and Recommendations

Modeling and validation of the performance of a hybrid NF/FO/RO membrane system for brackish water desalination was described in the first part. The feasibility of coupling this hybrid desalination system with renewable energy sources and determining the best coupling option was investigated and the cost of the product waster was estimated in the second part of the work. The following points are the main outcomes of the work, which is followed by recommendations for future work.

## 5.1 Conclusions

- A model was developed to determine the energy requirements of the hybrid NF/FO/RO process and the related processes. The specific energy consumption of the hybrid membrane system in Wadi Dawasir, Qassim and Tabuk was 2.3, 2.48 and 2.76 $kWh/m^3$, respectively.
- Different coupling options between the hybrid membrane system and different configurations of solar and wind energies, and different operation scenarios were studied including different operation periods and portions of energy utilized from different renewable energy sources, and all those studied coupling options and operation scenarios were compared and the best option in each case was determined.

- For the system in Wadi Dawasir, the best option was Diesel/Wind with a COE of 0.086 kWh/$m^3$, NPC of 7.42 M$, a drop in emissions of 45%, and a renewable energy fraction of 57%. For the system in Qassim, the best option was Diesel/PV with a COE of 0.089 kWh/$m^3$, NPC of 13.31 M$, a renewable energy fraction of 4%, and a drop in emissions of 7%. For the system in Tabuk, the best option was Diesel/PV with a COE of 0.087 kWh/$m^3$, NPC of 14.82 M$, a drop in emissions of 9%, and a renewable energy fraction of 5%.
- The product water cost for the systems in Wadi Dawasir, Qassim, and Tabuk is 0.61, 0.56, and 0.55 $/$m^3$, respectively.
- Optimization of the NF system alone, found that higher the recovery ratio, the lower the SEC and hence the highest RR that results in the desired product water concentration is the best. For the overall system, two points of interest were identified. One gives the lowest SEC (1.38 kWh/$m^3$) at a product concentration of 1058 and the other gives the lowest product concentration (1055 mg/l) at an SEC of 1.35 kWh/$m^3$.

## 5.2 Recommendations

- Study the feasibility of replacing the batteries with a water storage tank to minimize the need for operation at night.
- Investigate the use of a method for draw solution concentration recovery other than RO.

# References


[1] "AQUASTAT - FAO's Information System on Water and Agriculture." [Online]. Available: http://www.fao.org/nr/water/aquastat/water_use/index.stm. [Accessed: 12-Jan-2018].

[2] H. T. El-Dessouky and H. M. Ettouney, *Fundamentals of Salt Water Desalination*. 2002.

[3] H. van der Vegt, I. Iliev, Q. Tannock, and S. Helm, "Desalination Technologies and the Use of Alternative Energies for Desalination," *Pat. Landsc. Rep. Desalin. Technol. Use Altern. Energies Desalin.*, no. November, p. 92, 2011.

[4] L. F. Greenlee, D. F. Lawler, B. D. Freeman, B. Marrot, and P. Moulin, "Reverse osmosis desalination: Water sources, technology, and today's challenges," *Water Res.*, vol. 43, no. 9, pp. 2317–2348, 2009.

[5] M. Wilf and C. Bartels, "Optimization of seawater RO systems design," *Desalination*, vol. 173, no. 1, pp. 1–12, Mar. 2005.

[6] A. D. Khawaji, I. K. Kutubkhanah, and J. M. Wie, "Advances in seawater desalination technologies," *Desalination*, vol. 221, no. 1–3, pp. 47–69, 2008.

[7] Y. Al-Wazzan, M. Safar, and A. Mesri, "Reverse osmosis brine staging treatment of subsurface water," *Desalination*, vol. 155, no. 2, pp. 141–151, Jun. 2003.

[8] Puretec, "Basics of Reverse Osmosis," pp. 1–14.

[9] S. Zhao, L. Zou, C. Y. Tang, and D. Mulcahy, "Recent developments in forward

osmosis: Opportunities and challenges," *J. Memb. Sci.*, vol. 396, pp. 1–21, 2012.

[10] J. R. McCutcheon, R. L. McGinnis, and M. Elimelech, "A novel ammonia-carbon dioxide forward (direct) osmosis desalination process," *Desalination*, vol. 174, no. 1, pp. 1–11, 2005.

[11] T. CATH, A. CHILDRESS, and M. ELIMELECH, "Forward osmosis: Principles, applications, and recent developments," *J. Memb. Sci.*, vol. 281, no. 1–2, pp. 70–87, 2006.

[12] K. Sutherland, "Developments in filtration: What is nanofiltration?," *Filtr. Sep.*, vol. 45, no. 8, pp. 32–35, 2008.

[13] X. L. Wang, C. Zhang, and P. Ouyang, "The possibility of separating saccharides from a NaCl solution by using nanofiltration in diafiltration mode," *J. Memb. Sci.*, vol. 204, no. 1–2, pp. 271–281, 2002.

[14] S. L. Li, C. Li, Y. S. Liu, X. L. Wang, and Z. A. Cao, "Separation of L-glutamine from fermentation broth by nanofiltration," *J. Memb. Sci.*, vol. 222, no. 1–2, pp. 191–201, 2003.

[15] D. X. Wang *et al.*, "Modeling the separation performance of nanofiltration membranes for the mixed salts solution with Mg2+ and Ca2+," *J. Memb. Sci.*, vol. 284, no. 1–2, pp. 384–392, 2006.

[16] J. Ratana et al., "Performance evaluation of nano- filtration membrane for treatment of effluents containing reactive dyes and salt," *Desalination*, vol. 130, no. 00, pp. 177–183, 2000.

[17] A. Ali, R. A. Tufa, F. Macedonio, E. Curcio, and E. Drioli, “Membrane technology in renewable-energy-driven desalination,” *Renew. Sustain. Energy Rev.*, vol. 81, no. April 2017, pp. 1–21, 2018.

[18] M. Isaka, “Water Desalination Using Renewable Energy,” *Irena - Iea-Etsap*, no. March, p. 24, 2012.

[19] M. A. Eltawil, Z. Zhengming, and L. Yuan, “A review of renewable energy technologies integrated with desalination systems,” *Renew. Sustain. Energy Rev.*, vol. 13, no. 9, pp. 2245–2262, 2009.

[20] Rodríguez-Girones, M. Rodríguez, J. Pérez, and J. Veza, “A systematic approach to desalination powered by solar, wind and geothermal energy sources,” *Proc. Mediterr. Conf. Renew. energy sources water Prod. Eur. Comm. EURORED Network, CRES, EDS*, pp. 20–25, 1996.

[21] M. Taher, A. Dinar, and J. Albiac, “Modeling water scarcity and droughts for policy adaptation to climate change in arid and semiarid regions,” *J. Hydrol.*, vol. 522, pp. 95–109, 2015.

[22] S. S. Shenvi, A. M. Isloor, and A. F. Ismail, “A review on RO membrane technology: Developments and challenges,” *Desalination*, vol. 368, pp. 10–26, 2015.

[23] Y. Ayyash, H. Imai, T. Yamada, T. Fukuda, Y. Yanaga, and T. Taniyama, “Performance of reverse osmosis membrane in Jeddah Phase I plant,” *Desalination*, vol. 96, no. 1–3, pp. 215–224, 1994.

[24] M. B. Baig and A. A. Al Kutbi, “Design features of a 20 migd SWRO desalination plant, Al Jubail, Saudi Arabia,” *Desalination*, vol. 118, no. 1–3, pp. 5–12, 1998.

[25] A. Al-Karaghouli and L. Kazmerski, “Economic and Technical Analysis of a Reverse-Osmosis Water Desalination Plant Using DEEP-3. 2 Software,” *J. Environ. Sci. Eng. A*, vol. 1, no. 3, pp. 318–328, 2012.

[26] D. Hasson, A. Drak, and R. Semiat, “Inception of CaSO4 scaling on RO membranes at various water recovery levels,” *Desalination*, vol. 139, no. 1–3, pp. 73–81, 2001.

[27] C. Fritzmann, J. Löwenberg, T. Wintgens, and T. Melin, “State-of-the-art of reverse osmosis desalination,” *Desalination*, vol. 216, no. 1–3, pp. 1–76, 2007.

[28] M. H. Oo and L. Song, “Effect of pH and ionic strength on boron removal by RO membranes,” *Desalination*, vol. 246, no. 1–3, pp. 605–612, 2009.

[29] I. Alameddine and M. El-Fadel, “Brine discharge from desalination plants: a modeling approach to an optimized outfall design,” *Desalination*, vol. 214, no. 1–3, pp. 241–260, 2007.

[30] J. R. Mccutcheon, R. L. Mcginnis, and M. Elimelech, “A novel ammonia--carbon dioxide forward ( direct ) osmosis desalination process,” vol. 174, pp. 1–11, 2005.

[31] R. L. Mcginnis and M. Elimelech, “Energy requirements of ammonia – carbon dioxide forward osmosis desalination,” vol. 207, pp. 370–382, 2007.

[32] R. L. McGinnis, N. T. Hancock, M. S. Nowosielski-Slepowron, and G. D. McGurgan, “Pilot demonstration of the NH3/CO2 forward osmosis desalination

process on high salinity brines," *Desalination*, vol. 312, pp. 67–74, 2013.

[33] J. R. McCutcheon, R. L. McGinnis, and M. Elimelech, "Desalination by ammonia-carbon dioxide forward osmosis: Influence of draw and feed solution concentrations on process performance," *J. Memb. Sci.*, vol. 278, no. 1–2, pp. 114–123, 2006.

[34] K. Lutchmiah, A. R. D. Verliefde, K. Roest, L. C. Rietveld, and E. R. Cornelissen, "Forward osmosis for application in wastewater treatment: A review," *Water Res.*, vol. 58, no. 0, pp. 179–197, 2014.

[35] E. M. Vrijenhoek and J. J. Waypa, "Arsenic removal from drinking water by a 'loose' nanofiltration membrane," *Desalination*, vol. 130, no. 3, pp. 265–277, 2000.

[36] Diem Xuan Vuong, "Two stage nanofiltration seawater desalination system," 7144511, 2006.

[37] S. Adham, R. Cheng, DX Vuong, and K. L. Wattier, "Long Beach's dual-stage NF beats single-stage SWRO," *Intl. Desalin. water reuse*, vol. 13, no. 3, pp. 18–21, 2003.

[38] D. Zhou, L. Zhu, Y. Fu, M. Zhu, and L. Xue, "Development of lower cost seawater desalination processes using nanofiltration technologies - A review," *Desalination*, vol. 376, no. 1219, pp. 109–116, 2015.

[39] D. L. Shaffer, N. Y. Yip, J. Gilron, and M. Elimelech, "Seawater desalination for agriculture by integrated forward and reverse osmosis: Improved product water

quality for potentially less energy," *J. Memb. Sci.*, vol. 415–416, pp. 1–8, 2012.

[40] Y. J. Choi, J. S. Choi, H. J. Oh, S. Lee, D. R. Yang, and J. H. Kim, "Toward a combined system of forward osmosis and reverse osmosis for seawater desalination," *Desalination*, vol. 247, no. 1–3, pp. 239–246, 2009.

[41] V. Yangali-Quintanilla, Z. Li, R. Valladares, Q. Li, and G. Amy, "Indirect desalination of Red Sea water with forward osmosis and low pressure reverse osmosis for water reuse," *Desalination*, vol. 280, no. 1–3, pp. 160–166, 2011.

[42] C. H. Tan and H. Y. Ng, "A novel hybrid forward osmosis - nanofiltration (FO-NF) process for seawater desalination: Draw solution selection and system configuration," *Desalin. Water Treat.*, vol. 13, no. 1–3, pp. 356–361, 2010.

[43] A. Altaee, G. Zaragoza, and H. R. van Tonningen, "Comparison between Forward Osmosis-Reverse Osmosis and Reverse Osmosis processes for seawater desalination," *Desalination*, vol. 336, no. 1, pp. 50–57, 2014.

[44] T. N. Bitaw, K. Park, and D. R. Yang, "Optimization on a new hybrid Forward osmosis-Electrodialysis-Reverse osmosis seawater desalination process," *Desalination*, vol. 398, pp. 265–281, 2016.

[45] A. Ghermandi and R. Messalem, "Solar-driven desalination with reverse osmosis: the state of the art," *Desalin. Water Treat.*, vol. 7, no. 1–3, pp. 285–296, Aug. 2012.

[46] A. M. Helal, S. A. Al-Malek, and E. S. Al-Katheeri, "Economic feasibility of alternative designs of a PV-RO desalination unit for remote areas in the United

Arab Emirates," *Desalination*, vol. 221, no. 1–3, pp. 1–16, 2008.

[47] E. S. Mohamed and G. Papadakis, "Design, simulation and economic analysis of a stand-alone reverse osmosis desalination unit powered by wind turbines and photovoltaics," *Desalination*, vol. 164, no. 1, pp. 87–97, 2004.

[48] W. He, Y. Wang, and M. H. Shaheed, "Stand-alone seawater RO (reverse osmosis) desalination powered by PV (photovoltaic) and PRO (pressure retarded osmosis)," *Energy*, vol. 86, pp. 423–435, 2015.

[49] A. Joyce, D. Loureiro, C. Rodrigues, and S. Castro, "Small reverse osmosis units using PV systems for water purification in rural places," *Desalination*, vol. 137, no. 1–3, pp. 39–44, 2001.

[50] S. Alawaji, M. S. Smiai, S. Rafique, and B. Stafford, "PV-powered water pumping and desalination plant for remote areas in Saudi Arabia," *Appl. Energy*, vol. 52, no. 2–3, pp. 283–289, Jan. 1995.

[51] W. Gocht *et al.*, "Decentralized desalination of brackish water by a directly coupled reverse-osmosis-photovoltaic-system - a pilot plant study in Jordan," *Renew. Energy*, vol. 14, no. 1–4, pp. 287–292, May 1998.

[52] E. S. Mohamed, G. Papadakis, E. Mathioulakis, and V. Belessiotis, "A direct coupled photovoltaic seawater reverse osmosis desalination system toward battery based systems — a technical and economical experimental comparative study," *Desalination*, vol. 221, no. 1–3, pp. 17–22, Mar. 2008.

[53] S. Bouguecha, B. Hamrouni, and M. Dhahbi, "Small scale desalination pilots

powered by renewable energy sources: case studies," *Desalination*, vol. 183, no. 1–3, pp. 151–165, Nov. 2005.

[54] B. S. Richards, D. P. S. CapÃo, and A. I. SchÄfer, "Renewable Energy Powered Membrane Technology. 2. The Effect of Energy Fluctuations on Performance of a Photovoltaic Hybrid Membrane System," *Environ. Sci. Technol.*, vol. 42, no. 12, pp. 4563–4569, Jun. 2008.

[55] ITN, "Photovoltaic Reverse Osmosis Desalination System," *Reclam. Manag. Water West*, no. 104, 2004.

[56] R. A. Khaydarov and R. R. Khaydarov, "Solar powered direct osmosis desalination," *Desalination*, vol. 217, no. 1–3, pp. 225–232, 2007.

[57] J. Schrier, "Ethanol concentration by forward osmosis with solar-regenerated draw solution," *Sol. Energy*, vol. 86, no. 5, pp. 1351–1358, 2012.

[58] M. Khayet, J. A. Sanmartino, M. Essalhi, M. C. García-Payo, and N. Hilal, "Modeling and optimization of a solar forward osmosis pilot plant by response surface methodology," *Sol. Energy*, vol. 137, pp. 290–302, 2016.

[59] P. McKenna, "Purifying the dirtiest waters, NovaNext," 2015. [Online]. Available: www.pbs.org/wgbh/nova/next/tech/forward-osmosis/. [Accessed: 05-Jan-2018].

[60] A. A. Monjezi, H. B. Mahood, and A. N. Campbell, "Regeneration of dimethyl ether as a draw solute in forward osmosis by utilising thermal energy from a solar pond," *Desalination*, vol. 415, pp. 104–114, 2017.

[61] G. Iaquaniello, A. Salladini, A. Mari, A. A. Mabrouk, and H. E. S. Fath,

"Concentrating solar power (CSP) system integrated with MED–RO hybrid desalination," *Desalination*, vol. 336, pp. 121–128, Mar. 2014.

[62] M. Hoyer, R. Haseneder, and J.-U. Repke, "Development of a hybrid water treatment process using forward osmosis with thermal regeneration of a surfactant draw solution," *Desalin. Water Treat.*, vol. 57, no. 59, pp. 28670–28683, Dec. 2016.

[63] A. N. A. Mabrouk and H. E. S. Fath, "Experimental study of high-performance hybrid NF-MSF desalination pilot test unit driven by renewable energy," *Desalin. Water Treat.*, vol. 51, no. 37–39, pp. 6895–6904, Nov. 2013.

[64] A. N. A. Mabrouk and H. E. S. Fath, "Techno-economic analysis of hybrid high performance MSF desalination plant with NF membrane," *Desalin. Water Treat.*, vol. 51, no. 4–6, pp. 844–856, Jan. 2013.

[65] O. A. Hamed, A. M. Hassan, K. Al-Shail, and M. A. Farooque, "Performance analysis of a trihybrid NF/RO/MSF desalination plant," *Desalin. Water Treat.*, vol. 1, no. 1–3, pp. 215–222, Jan. 2009.

[66] "EES: Engineering Equation Solver | F-Chart Software : Engineering Software." [Online]. Available: http://www.fchart.com/ees/. [Accessed: 09-Jan-2018].

[67] "HOMER Pro - Microgrid Software for Designing Optimized Hybrid Microgrids." [Online]. Available: https://www.homerenergy.com/homer-pro.html. [Accessed: 09-Jan-2018].

[68] A. Altaee and N. Hilal, "High recovery rate NF – FO – RO hybrid system for

inland brackish water treatment," vol. 363, pp. 19–25, 2015.

[69] C. Garcia, F. Molina, and D. Zarzo, "7 year operation of a BWRO plant with raw water from a coastal aquifer for agricultural irrigation," *Desalin. Water Treat.*, vol. 31, no. 1–3, pp. 331–338, Jul. 2011.

# Vitae


Name :MOHAMMED FAISAL MUSA ABDELMAHMOUD

Nationality :Sudanese

Date of Birth :11/29/1990

Email :muhafaisal075@gmail.com

Address :Khartoum, Sudan, postal code:12213


Academic Background : **M. Sc. (Mechanical Engineering), May, 2018**

King Fahd University of Petroleum and minerals

Dhahran, Saudi Arabia

**B. Sc. (Mechanical Engineering), October 2012**

University of Khartoum

Khartoum, Sudan

Publications : Mohammed F. Musa & Fahad Al-Sulaiman, “Renewable Energy-Powered Hybrid NF/FO/RO Membrane System for Brackish Water Desalination, ” journal paper, to be submitted.